coexistent proliferative epidermal lesions, such as condyloma acuminatum, Bowen's disease, and squamous cell carcinoma, but not in adjacent EMPD areas [3,9,10]. Therefore, HPV infection in these cases is more likely coincidental than causal in the pathogenesis of EMPD, although the precise relationship still needs to be elucidated.

Our findings provide further evidence that HPV infection is unlikely to contribute to the carcinogenesis of EMPD. However, further investigation is required to determine whether or not there is an association between EMPD and other types of HPV that were not detected by the methods used in this study.

References

[1] Snow SN, Desouky S, Lo JS, Kurtycz D. Failure to detect human papillomavirus DNA in extramammary Paget's disease. Cancer 1992;69:249–51.
[2] Takata M, Hatta N, Takehara K. Tumor cells of extramammary Paget's disease do not show either p53 mutation or allelic loss at several selected loci implicated in other cancers. Br J Cancer 1997;76:904–8.
[3] Brainard JA, Hart WR. Proliferative epidermal lesions associated with anogenital Paget's disease. Am J Surg Pathol 2000;24:543–52.
[4] Orlandi A, Piccione E, Francesconi A, Spagnoli LG. Simultaneous vulvar intraepithelial neoplasia and Paget's disease: report of two cases. Int J Gynecol Cancer 2001;11:224–8.
[5] Murao K, Kubo Y, Takiwaki H, Matsumoto K, Arase S. Bowen's disease on the sole: $p16^{INK4a}$ overexpression associated with human papillomavirus type 16. Br J Dermatol 2005;152:170–3.
[6] Karlsen F, Kalantari M, Jenkins A, Pettersen E, Kristensen G, Holm R, et al. Use of multiple PCR primer sets for optimal detection of human papillomavirus. J Clin Microbiol 1996;34:2095–100.
[7] Perrons C, Kleter B, Jelley R, Jalal H, Quint W, Tedder R. Detection and genotyping of human papillomavirus DNA by SPF10 and MY09/11 primer in cervical cells taken from women attending a colposcopy clinic. J Med Virol 2002;67:246–52.
[8] Kazakov DV, Nemcova J, Mikyskova I, Belousova IE, Vazmitel M, Michal M. Human papillomavirus in lesions of anogenital mammary-like glands. Int J Gynecol Pathol 2007;26:475–80.
[9] Egawa K, Honda Y. Simultaneous human papillomavirus 6 (HPV6)–positive condyloma acuminatum, HPV 31-positive Bowen's disease, and non HPV-associated extramammary Paget's disease coexisting within an area presenting clinically as condyloma acuminatum. Am J Dermatopathol 2005;27:439–42.
[10] Honda Y, Egawa K. Extramammary Paget's disease not only mimicking but also accompanying condyloma acuminatum. Dermatology 2005;210:315–8.

Kazutoshi Murao*
Yoshiaki Kubo
Tsuyoshi Ishigami
Seiji Arase
Department of Dermatology, Institute of Health Biosciences, The University of Tokushima Graduate School, 15-18-3 Kuramoto-cho, Tokushima, Japan

*Corresponding author. Tel.: +81 866 33 7154; fax: +81 886 32 0434
E-mail address: kmurao@clin.med.tokushima-u.ac.jp (K. Murao)

30 March 2010

doi:10.1016/j.jdermsci.2010.07.002

Letter to the Editor

Chromosome 11q13.5 variant: No association with atopic eczema in the Japanese population

Dear Sir,

A single nucleotide polymorphism (SNP) on chromosome 11q13.5 [rs7927894] has been attracting great attention since Esparza-Gordillo et al. [1] reported highly significant association of a common variant of rs7927894 with atopic eczema (AE) in the German population. In the report, approximately 13% of individuals are homozygous for the SNP and their risk of developing AE is 1.47 times that of noncarriers. Very recently, O'Regan et al. [2] further published interesting results on the association between rs7927894 and AE in a collection of Irish children with moderate-to-severe AE and Irish controls. The association between rs7927894 and AE was replicated in the Irish population ($p = 0.0025$, Chi-square test; odds ratio (OR) = 1.27, 95% confidence interval (CI) 1.09–1.49). Additional analyses performed to test the statistical significance of the rs7927894 SNP having controlled for the presence/absence of the strongly significant *FLG* null genotype indicated that rs7927894 still shows a statistically significant effect ($p = 0.0025$) with an OR of 1.22 (95% CI 1.02–1.26) [2]. Tests for interaction between each of the *FLG* and rs7927894 risk alleles showed no evidence of statistically significant epistatic effects [2]. The rs7927894 association was independent of the well-established *FLG* risk alleles and may be multiplicative in its effects.

In order to clarify whether this common variant is associated with AE also in the Japanese population or not, we evaluated the association between rs7927894 and AE in an cohort of 194 Japanese AE patients we had collected to date and 113 unrelated Japanese control individuals. All the AE patients had been diagnosed with AE based on widely recognized diagnostic criteria [3] or their parents reported a dermatologist's diagnosis of AE (at least once). Majority of AE patients and control individuals were identical to those in a previous study [4]. Using genomic DNA, AE patients and control individuals were screened for the variant allele of rs7927894 on chromosome 11q13, by direct DNA sequencing. In addition, the AE patients and the control individuals were screened for eight *FLG* mutations previously identified in the Japanese population, by restriction enzyme digestion, fluorescent PCR and/or direct DNA sequencing as described previously [4,5].

Case–control association analyses were performed for the variant using Fisher's exact test. In addition, we performed case–control statistical analysis for the common variant allele of rs7927894 after stratification for *FLG* mutations. The rs7927894 on chromosome 11q13 genotype data in the Japanese AE case series and ethnically matched population control series are summarized in Table 1. All alleles were observed to be in normal Hardy–Weinberg equilibrium.

Here we demonstrate that 22.7% and 1.5% of the patients in our Japanese AE case series are heterozygous and homozygous for rs7927894[T], respectively (combined rs7927894[T] allele frequency = 0.129, $n = 388$) (Table 1). rs7927894[T] is also carried by 23.0% of the Japanese control individuals (combined minor allele frequency = 0.115, $n = 226$). There is no statistically significant association between the rs7927894[T] and AE.

After stratification for *FLG* mutations previously identified in the Japanese population, 26.0% and 4.0% of our Japanese AE case series with *FLG* mutations are heterozygous and homozygous for rs7927894[T] (combined rs7927894[T] allele frequency = 0.17, $n = 100$). 21.5% and 0.7% of the Japanese AE patients without *FLG* mutations are heterozygous and homozygous for rs7927894[T] (combined rs7927894[T] allele frequency = 0.11, $n = 288$). There is no statistically significant association between the rs7927894[T] and AE without *FLG* mutations or rs7927894[T] and AE with *FLG* mutations (Fisher's exact test $p = 0.338$). Furthermore, interaction

Table 1
Results of the 11q13.5 SNP and the prevalent *FLG* mutations in 194 Japanese eczema cases and 113 individuals from Japanese control population.

	Eczema cases			Control		
	Total	*FLG* (+)	*FLG* (−)	Total	*FLG* (+)	*FLG* (−)
C/C	147 (75.8%)	35 (70.0%)	112 (77.8%)	87 (77.0%)	2 (50.0%)	85 (78.0%)
C/T	44 (22.7%)	13 (26.0%)	31 (21.5%)	26 (23.0%)	2 (50.0%)	24 (22.0%)
T/T	3 (1.5%)	2 (4.0%)	1 (0.7%)	0 (0%)	0 (0%)	0 (0%)
Total	194	50	144	113	4	109

FLG (+), with *FLG* mutation(s); *FLG* (−), without any *FLG* mutation. Combined rs7927894[T] allele frequency, 0.129 (AE patients, $n = 388$); 0.115 (control individuals, $n = 226$); 0.17 (AE patients with *FLG* mutation(s), $n = 100$); 0.115 (AE patients without *FLG* mutation(s), $n = 288$).

Table 2
Cross-classification of genotypes of rs7927894 and *FLG* used for the interaction analysis.

Genotype		Cases			Controls		
		rs7927894			rs7927894		
		AA	AA	Aa	AA	Aa	aa
R501X	AA	147	44	3	87	26	0
	Aa	0	0	0	0	0	0
	aa	0	0	0	0	0	0
3321delA	AA	141	42	2	87	25	0
	Aa	6	2	1	0	1	0
	aa	0	0	0	0	0	0
S1695X	AA	147	44	3	86	26	0
	Aa	0	0	0	1	0	0
	aa	0	0	0	0	0	0
Q1701X	AA	144	44	3	87	26	0
	Aa	3	0	0	0	0	0
	aa	0	0	0	0	0	0
S2554X	AA	141	41	3	87	26	0
	Aa	6	3	0	0	0	0
	aa	0	0	0	0	0	0
S2889X	AA	133	36	2	86	25	0
	Aa	14	8	1	1	1	0
	Aa	0	0	0	0	0	0
S3296X	AA	141	43	3	87	26	0
	Aa	6	1	0	0	0	0
	Aa	0	0	0	0	0	0
K4022X	AA	144	43	3	87	26	0
	Aa	3	1	0	0	0	0
	Aa	0	0	0	0	0	0
Combined *FLG* null genotype	AA	109	31	1	85	24	0
	Aa	35	13	2	2	2	0
	Aa	0	0	0	0	0	0

AA, wild-type homozygous individuals for each genetic variant; Aa, wild-type/mutant heterozygous individuals; aa, individuals who are homozygous for each of the genetic variants tested.

between each of the *FLG* and rs7927894 risk alleles based on the cross-classification of genotypes in Table 2 showed no apparent epistatic effects.

rs7927894 is located in an intergenic region 38 kb downstream of *C11orf30* (chromosome 11 open reading frame 30) and 68 kb upstream of *LRRC322* (leucine rich repeat containing 32). Both *C11orf30* and *LRRC322* are ubiquitously expressed including skin and peripheral blood lymphocytes [1]. By genome-wide association study for global mRNA expression in lymphoblastoid cell lines from asthmatic children, there was no evidence for a *cis*-regulatory effect of rs7927894 [6]. Thus, regulatory role of rs7927894 on *C11orf30* and *LRRC322* gene expression is questionable. However, we cannot exclude the possibility of a pathogenetic link of rs7927894 to atopic eczema via *C11orf30* and *LRRC322* gene expression in the skin.

Our case–control study in the Japanese population did not confirm the result of Esparza-Gordillo et al. [1] or O'Regan et al. [2] that rs7927894 is at increased risk for AE. The association of rs7927894 with AE was reported in the European population, i.e. in the German population by Esparza-Gordillo et al. [1] and in the Irish population by O'Regan et al. [2]. The present data suggest that the association of rs7927894 with AE established in the European populations is not in the Asian populations, at least in the Japanese population.

Acknowledgments

We thank Ms. Yuki Miyamura and Ms. Kaori Sakai for the fine technical assistance. This work was supported in part by Grants-in-Aid from the Ministry of Education, Science, Sports, and Culture of Japan to M. Akiyama (Kiban B 20390304), a grant from Ministry of Health, Labour and Welfare of Japan (Health and Labour Sciences Research Grants; Research on Intractable Disease: H21-047) to M. Akiyama and a Health and Labour Sciences Research Grant (Research on Allergic diseases and Immunology; H21-Meneki-Ippan-003) to H. Shimizu.

References

[1] Esparza-Gordillo J, Weidinger S, Fölster-Holst R, Bauerfeind A, Ruschendorf F, Patone G, et al. A common variant on chromosome 11q13 is associated with atopic dermatitis. Nat Genet 2009;41:596–601.
[2] O'Regan GM, Campbell LE, Cordell HJ, Irvine AD, McLean WHI, Brown SJ. Chromosome 11q13.5 variant associated with childhood eczema: an effect supplementary to filaggrin mutations. J Allergy Clin Immunol 2010;125: 170–4.
[3] Hannifin JM, Rajka G. Diagnostic features of atopic dermatitis. Acta Derm Venereol 1980;92:44–7.
[4] Nemoto-Hasebe I, Akiyama M, Nomura T, Sandilands A, McLean WHI, Shimizu H. FLG mutation p.Lys4021X in the C-terminal imperfect filaggrin repeat in Japanese atopic eczema patients. Br J Dermatol 2009;161:1387–90.
[5] Nomura T, Sandilands A, Akiyama M, Sakai K, Ota M, Sugiura H, et al. Unique mutations in the filaggrin gene in Japanese patients with ichthyosis vulgaris and atopic dermatitis. J Allergy Clin Immunol 2007;119:434–40.
[6] Dixon AL, Liang L, Moffatt MF, Chen W, Heath S, Wong KC, et al. A genome-wide association study of global gene expression. Nat Genet 2007;39:1202–7.

Yukiko Nomura
Department of Dermatology, Hokkaido University Graduate School of Medicine, North 15 West 7, Sapporo, Hokkaido 060-8638, Japan

Masashi Akiyama*
Department of Dermatology, Hokkaido University Graduate School of Medicine, North 15 West 7, Sapporo, Hokkaido 060-8638, Japan

Toshifumi Nomura[a,b]
[a]*Department of Dermatology, Hokkaido University Graduate School of Medicine, North 15 West 7, Sapporo, Hokkaido 060-8638, Japan*

[b]*Epithelial Genetics Group, Division of Molecular Medicine, University of Dundee, Colleges of Life Sciences and Medicine, Dentistry & Nursing, Dundee, UK*

Ikue Nemoto-Hasebe
Department of Dermatology, Hokkaido University Graduate School of Medicine, North 15 West 7, Sapporo, Hokkaido 060-8638, Japan

Riichiro Abe
Department of Dermatology, Hokkaido University Graduate School of Medicine, North 15 West 7, Sapporo, Hokkaido 060-8638, Japan

W.H. Irwin McLean
Epithelial Genetics Group, Division of Molecular Medicine, University of Dundee, Colleges of Life Sciences and Medicine, Dentistry & Nursing, Dundee, UK

Hiroshi Shimizu
Department of Dermatology, Hokkaido University Graduate School of Medicine, North 15 West 7, Sapporo, Hokkaido 060-8638, Japan

*Corresponding author. Tel.: +81 11 706 7387;
fax: +81 11 706 7820
E-mail address: akiyama@med.hokudai.ac.jp
(M. Akiyama)

8 February 2010

doi:10.1016/j.jdermsci.2010.06.010

Bone marrow transplantation restores epidermal basement membrane protein expression and rescues epidermolysis bullosa model mice

Yasuyuki Fujita[a], Riichiro Abe[a,1], Daisuke Inokuma[a], Mikako Sasaki[a], Daichi Hoshina[a], Ken Natsuga[a], Wataru Nishie[a], James R. McMillan[a], Hideki Nakamura[a], Tadamichi Shimizu[b], Masashi Akiyama[a], Daisuke Sawamura[c], and Hiroshi Shimizu[a,1]

[a]Department of Dermatology, Hokkaido University Graduate School of Medicine, Sapporo 060-8638, Japan; [b]Department of Dermatology, Toyama University Graduate School of Medicine and Pharmaceutical Sciences, Toyama 930-0194, Japan; and [c]Department of Dermatology, Hirosaki University Graduate School of Medicine, Hirosaki 036-8562, Japan

Edited* by Douglas Lowy, National Institutes of Health, Bethesda, MD, and approved June 24, 2010 (received for review January 4, 2010)

Attempts to treat congenital protein deficiencies using bone marrow-derived cells have been reported. These efforts have been based on the concepts of stem cell plasticity. However, it is considered more difficult to restore structural proteins than to restore secretory enzymes. This study aims to clarify whether bone marrow transplantation (BMT) treatment can rescue epidermolysis bullosa (EB) caused by defects in keratinocyte structural proteins. BMT treatment of adult collagen XVII (Col17) knockout mice induced donor-derived keratinocytes and Col17 expression associated with the recovery of hemidesmosomal structure and better skin manifestations, as well improving the survival rate. Both hematopoietic and mesenchymal stem cells have the potential to produce Col17 in the BMT treatment model. Furthermore, human cord blood CD34$^+$ cells also differentiated into keratinocytes and expressed human skin component proteins in transplanted immunocompromised (NOD/SCID/γ_c^{null}) mice. The current conventional BMT techniques have significant potential as a systemic therapeutic approach for the treatment of human EB.

hematopoietic stem cells | type XVII collagen

Bone marrow-derived cells, including hematopoietic stem cells and mesenchymal stem cells, have been reported to play a significant role in the recovery of various impaired organs (1–8). Although some papers have reported that "transdifferentiation" of circulating hematopoietic stem cells is an extremely rare event (9), previous reports have shown that expression of systemic enzymes and certain secreted factors can be recovered after bone marrow transplantation (BMT) (10).

Epidermolysis bullosa (EB) comprises a group of genodermatoses, which are caused by mutations in one of the genes encoding anchor proteins that stabilize the basement membrane zone (BMZ) of the skin and mucous membranes (11). Collagen XVII (COL17) is a transmembrane component of hemidesmosomal adhesion structures anchoring cells to the BMZ. *COL17* is the gene underlying non-Herlitz junctional EB in humans, a disorder that causes severe skin fragility, hair loss, growth retardation, and enamel hypoplasia (11). There is no effective treatment for EB other than palliative care. Gene-treated cultured autografting, reported by Mavilio et al. (12), is a promising therapeutic approach for junctional EB. However, its effects are limited to the area of application, in addition to the ethical and safety problems of using viruses for gene correction, even if the recent development of lentiviral vectors with favorable safety might be able to avoid the risks of gene augmentation with traditional retroviral constructs (13). Therefore, systemic and ethically safer therapies would be preferable.

Previous work reported that cells of human or murine origin do home to the skin, such as in graft-versus-host disease in humans (14) and epithelial progenitors in murine bone marrow (15). Our group reported that donor-derived keratinocytes could be identified at wound sites in a BMT model (16). This suggests that BMT techniques have the potential to provide functional keratinocytes over the entire skin surface. The current study investigates whether BM-derived cells can differentiate into donor-derived keratinocytes and subsequently produce detectable COL17 protein after BMT, with the ultimate goal of improving the clinical phenotype and contributing to long-term survival in our model mice.

Results

Donor BM-Derived Cells Express Col17 Protein in the BMZ in Recipient Mouse Skin. To investigate whether BM-derived keratinocytes can produce skin component proteins, we transplanted BM-derived cells of C57BL/6 mice expressing *human COL17* (*hCOL17*) driven by the keratin 14 promoter (*COL17*$^{m+/+,h+}$) into wild-type C57BL/6 mice in the first set of experiments. Detection of hCOL17 protein in the epithelized recipient skin would indicate that donor BM-derived cells had differentiated into keratinocytes. Immunohistochemical analysis revealed hCOL17 protein expression in the BMZ within the wounded area for four out of the eight BMT-treated C57BL/6 mice (Fig. 1*A*). RT-PCR analysis also showed evidence of *hCOL17* mRNA expression in five out of the eight treated mice (Fig. 1*B*).

We subsequently performed another BMT experiment: BM-derived cells from GFP$^+$ Tg mice were transplanted into COL17-humanized (*COL17*$^{m-/-,h+}$) mice (Fig. S1) (17). In this experimental pattern, BM-derived cells that differentiated into keratinocytes in the host mice were found to have the potential to produce mCol17 protein. BM-derived nonhematopoietic cells expressing GFP$^+$ CD45$^-$ were sparsely observed, accounting for $1.83 \pm 0.82\%$ ($n = 5$) of the basal layer cells (Fig. 1*C*). Aggregated GFP$^+$ cytokeratin$^+$ cells were also found in the basal cell layer (Fig. 1*D*). Epithelized skin areas in this experiment demonstrated mCol17 protein expression, although unwounded areas of the transplanted *COL17*$^{m-/-,h+}$ mice failed to express that protein (Fig. 1*E*). This mCol17 expression lasted at least 9 mo after wound formation in two out of the three investigated mice (Fig. S2). RT-PCR analysis also revealed the expression of *mCol17* mRNA in epithelized skin from four of the five transplanted mice, indicating that the BM-derived epidermal cells were able to express active *mCol17* (Fig. 1*F*).

Author contributions: Y.F., R.A., D.I., W.N., T.S., M.A., D.S., and H.S. designed research; Y.F., D.I., M.S., D.H., K.N., W.N., J.R.M., H.N., and D.S. performed research; K.N. and W.N. contributed new reagents/analytic tools; and Y.F., R.A., M.S., J.R.M., M.A., and H.S. analyzed data; and Y.F. and R.A. wrote the paper.

The authors declare no conflict of interest.

*This Direct Submission article had a prearranged editor.

[1]To whom correspondence may be addressed. E-mail: aberi@med.hokudai.ac.jp or shimizu@med.hokudai.ac.jp.

This article contains supporting information online at www.pnas.org/lookup/suppl/doi:10.1073/pnas.1000044107/-/DCSupplemental.

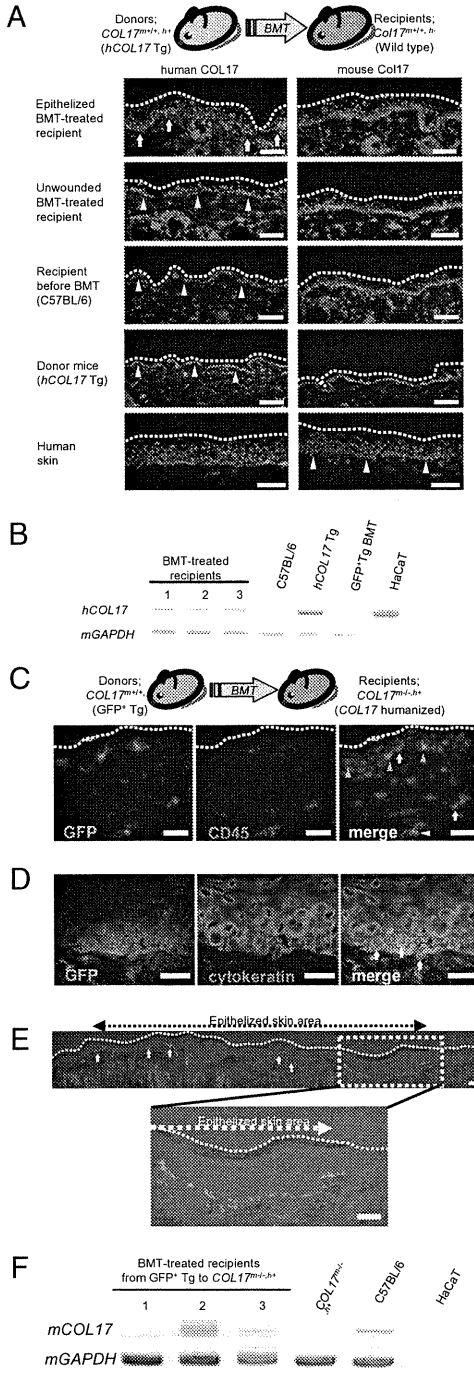

Fig. 1. BMT-induced donor cell-derived COL17 in the epithelized skin tissue. (*A*) The donor-derived hCOL17 expression is observed in the epithelized skin areas of BMT-treated C57BL/6 recipients (yellow arrows). Green: mCol17 (KT4.2) or hCOL17 (D20); red: nuclei; broken lines: skin surface; arrowheads: BMZ. (Scale bars: 50 μm.) (*B*) Representative RT-PCR analysis for *hCOL17* expression reveals positive bands in BMT-treated C57BL/6 recipients. All RNA samples were extracted from full-thickness skin biopsies, except for HaCaT from cultured cells. (*C*) Immunohistochemical analysis of the BMT-treated $COL17^{m-/-,\ h+}$ skin tissue demonstrates donor-derived GFP^+ $CD45^+$ blood cells (yellow arrowheads) and recipient-derived GFP^- $CD45^+$ cells (yellow arrow). Donor-derived GFP^+ $CD45^-$ (green arrowheads) cells are sporadically noted in the epidermis. (Scale bars: 20 μm.) (*D*) Aggregated donor-derived GFP^+ cells in the basal cell layer are noted, some of which also express cytokeratin (white arrows). These cells are thought to be donor-derived keratinocytes. (Scale bars: 20 μm.) (*E*) The skin of the recipients shows sporadic, linear deposition of mCol17 (arrows). The deposition is limited to the epithelized skin area with acanthosis. (*Upper*) The entire consolidated image. (*Lower*) Higher magnification. (Scale bars: 50 μm.) (*F*) RT-PCR analysis shows the recovery of *mCol17* mRNA in two out of three representative mice (lanes 2 and 3).

BM-Derived Cells Supply Deficient Col17 Protein in the Col17 Knockout EB Model Mice. Our group recently established non-Herlitz junctional EB model mice ($COL17^{m-/-}$) as a result of homozygous ablation of the Col17 gene (17). Unlike EB model mice reported by other researchers, our model has allowed us to obtain adult $COL17^{m-/-}$ mice that can be used for various therapeutic strategies (Fig. S3). We speculated that mCol17 protein would be reintroduced by administering BM-derived cells from BMT treatments into $COL17^{m-/-}$ EB model mice. We transplanted BM cells of the GFP^+ Tg mice into the $COL17^{m-/-}$ mice. All of the mice obtained hematopoietic chimeras (710. ± 4.0%, $n = 21$). Immunohistochemical analysis revealed sporadic GFP^+ cells in the basal cell layer of the epidermis, accounting for 1.08 ± 0.39% of the basal cells ($n = 11$). GFP^+ $CD45^-$ cells including cytokeratin$^+$ epidermal keratinocytes were also found (0.26% ± 0.08% of basal cells) (Fig. 2*A* and Fig. S4). Linear deposition of mCol17 along the BMZ, and GFP^+ cells above the mCol17 staining were observed, accounting for 14.7 ± 3.0% ($n = 11$) of the epithelized area (Fig. 2*B*). Also, a 180-kDa mCol17 protein was detected in Western blotting (Fig. 2*C*). One out of three mice showed positive mCol17 immunohistochemically in unwounded skin from the back (Fig. S5*A*). Eight out of nine BMT-treated mice showed positive *mCol17* mRNA in the epithelized skin tissues. Compared with unwounded skin, epithelized areas of skin tended to show *mCol17* mRNA expression more frequently (Fig. S5*B*). We also performed RT-PCR analysis on the epithelized areas of BMT-treated $COL17^{m-/-}$ mice from the epidermis and the dermis by detaching each side enzymatically; this revealed positivity only on the epidermal side (Fig. 2*D*). Next, we sorted GFP^+ cells from the single-cell suspension of epithelized epidermal cells. A portion of the suspended epidermal cells showed GFP (1.24 ± 0.12%, $n = 4$; Fig. S6), and mRNA expression specific to epidermal keratinocytes was detected from the extract of the GFP^+ epidermal cells. These cells also expressed *mCol17* mRNA in three out of the four investigated mice (Fig. 2*E*). To rule out the possibility that cell fusion was occurring between BM cells and original keratinocytes in the $COL17^{m-/-}$ mice, we performed FISH analysis in a sex-mismatched BMT model. Several fused cells with XXXY chromosomes in the same nucleus were found in the deep dermis of the epithelized skin (Fig. 2*F*). Conversely, no fused cells were found in the epidermis of the samples we investigated, whereas 50 of 1,793 basal cells (2.79%) showed donor-derived XY chromosomes. To investigate the restoration of COL17 expression and its effect on restoring normal BMZ structure, we performed electron microscopic analysis. In the BMT-treated $COL17^{m-/-}$ mice, a portion of the basal cells had mature hemidesmosomes (Fig. 2*G*). The average thickness of outer plaques of hemidesmosomes was 79.7 ± 3.2 nm in the wild-type mice, 45.1 ± 1.4 nm in the untreated $COL17^{m-/-}$ mice, and 61.1 ± 1.9 nm in the BMT-treated $COL17^{m-/-}$ mice ($P < 0.01$). To exclude the nonspecific effects of bone marrow infusion, a mixture of lineage$^+$ differentiated GFP^+ BM cells and lineage$^-$ $COL17^{m-/-}$ BM cells was transplanted into the $COL17^{m-/-}$ mice. No Col17 expression of mRNA and protein were detected in the epithelized skin ($n = 3$).

Col17 Knockout Mice Exhibit Less Severe Clinical Manifestations and Better Survival Prognosis After BMT than Untreated Mice. To investigate the change in vulnerability to friction in skin that resulted from the restoration of Col17, we rubbed the back of each mouse (18). The BMT-treated mice ($n = 6$) significantly showed formation of smaller erosions compared with the untreated mice ($n = 4$) (Fig. 3*A*). Although our $COL17^{m-/-}$ mice survived longer than previously reported EB models, only 12.5% of the mice survived to 1 mo, approximately half of which died within the following 3 mo (17). Surprisingly, 16 out of the 20 transplanted $COL17^{m-/-}$ mice survived to 100 d after BMT (transplanted on d 35 after birth), whereas only 7 out of the 17 untreated $COL17^{m-/-}$ mice survived to

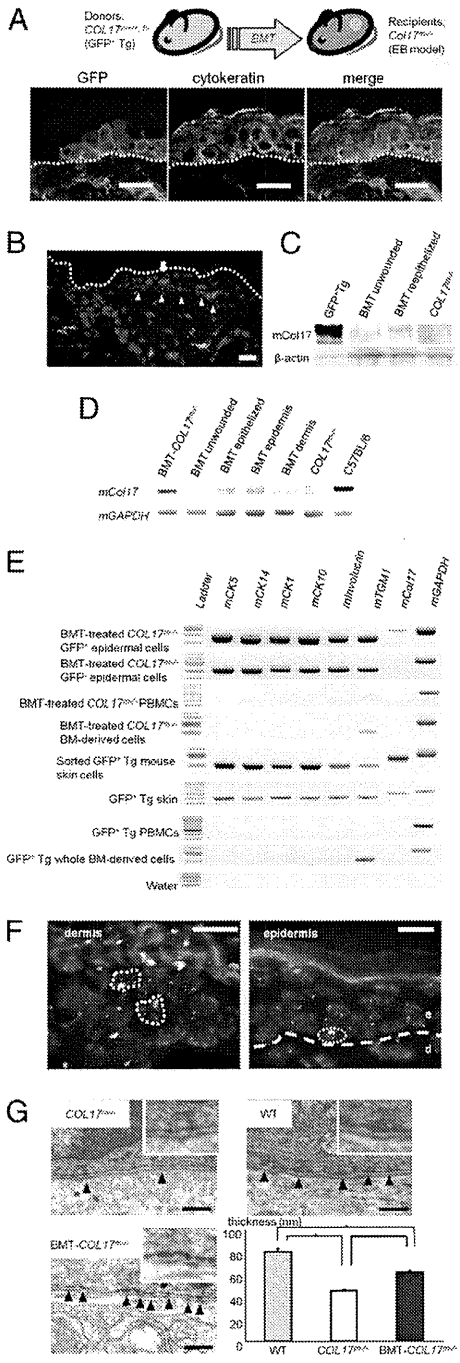

Fig. 2. BMT treatments induce functional mCol17 in *COL17*$^{m-/-}$ junctional EB model mice. (*A*) In the epithelized skin tissue of BMT-treated mice, a cluster of GFP$^+$ cytokeratin$^+$ basal cells is observed. Green: GFP; blue: nuclei; broken lines: skin surface. (Scale bars: 10 μm.) (*B*) Sporadic GFP$^+$ cells (green) are shown in the epithelized skin of the recipients (arrow). Furthermore, linear staining of mCol17 is detected in the BMZ (red, KT4.2, arrowheads). (Scale bars: 20 μm.) (*C*) Western blotting analysis reveals the expression of mCol17 in the epithelized area of the BMT-treated *COL17*$^{m-/-}$ mouse (lane 3), and a weak band is seen in unwounded skin of a BMT-treated *COL17*$^{m-/-}$ mouse (lane 2). β-actin: loading control. (*D*) The expression of *mCol17* is detected only in the epithelized skin and not in the unwounded skin area. Also, the expression is limited to the epidermis side of the epithelized skin. (*E*) The sorted GFP$^+$ single epidermal cells of BMT-treated *COL17*$^{m-/-}$ mice express various keratinocyte-specific mRNAs as well as *mCol17*. Sorted GFP$^-$ cells express these mRNAs, other than that of mCol17. (*F*) No fused cells are apparent in the epidermis, although donor-derived XY cells are sparsely shown. Sporadic fused cells with XXXY chromosomes are observed in the deep dermis. Dashed circles indicate the border of the nucleus. e: epidermis; d: dermis. (Scale bars: 10 μm.) (*G*) The epithelized skin of *COL17*$^{m-/-}$ mice has hypoplastic hemidesmosomes with thin, poorly formed inner/outer plaques (arrowheads). In BMT-treated *COL17*$^{m-/-}$ mice, hemidesmosomes with mature plaques are seen. (Scale bars: 500 nm.) *$P < 0.01$.

d 135 after birth. The survival outcomes were 73.7% for the transplanted group and 27.5% for the untreated group at d 200 after BMT (Fig. 3*B*). The BMT technique brought significant therapeutic benefits to the *COL17*$^{m-/-}$ EB model mice.

The untreated adult *COL17*$^{m-/-}$ EB model mice showed spontaneous erosions, ulcers, nail deformity, hair loss, and hair graying similar to those seen in human junctional EB patients lacking *COL17* (17). The erosions were especially severe in the genital regions (Fig. 3*C*). The BMT-treated *COL17*$^{m-/-}$ mice showed improvements to clinical manifestations, with fewer spontaneous erosions than for the untreated *COL17*$^{m-/-}$ mice and BMT-control *COL17*$^{m-/-}$ mice (*COL17*$^{m-/-}$ mice as donors). The improvements were particularly marked in the genital regions (Fig. S7).

Both Hematopoietic and Mesenchymal Stem Cells Contribute to the Expression of Col17. Because BM cells consist of various differentiated hematopoietic cells and stem cells, there is the question of which type of BM-derived stem cells produced the Col17 and caused clinical improvement in the *COL17*$^{m-/-}$ EB model mice. We obtained hematopoietic stem cells (HSCs) and multipotent mesenchymal stromal cells (MSCs) from GFP$^+$ Tg mice, following transplantation of each type of stem cell into *COL17*$^{m-/-}$ mice with whole *COL17*$^{m-/-}$ BM-derived cells as supporting cells (Fig. 4*A*). Four weeks after BMT, we confirmed partial chimerism (37.0 ± 13.7%, $n = 5$) of GFP in peripheral blood of BMT-treated mice with GFP$^+$ HSCs (HSC-BMT mice), whereas no GFP$^+$ peripheral blood cells were detected in BMT-treated mice with GFP$^+$ MSCs (MSC-BMT mice, $n = 4$) (Fig. S8). Immunohistochemical analysis revealed sparse GFP$^+$ cytokeratin$^+$ keratinocytes in the skin of the HSC- and MSC-BMT mice (Fig. 4*B*). Both HSCs and MSCs were found to have the potential to produce mCol17 as observed immunohistochemically; three out of five HSC-BMT mice and two out of four MSC-BMT mice showed positive mCol17 (Fig. 4*C*). RT-PCR analysis also demonstrated the expression of *mCol17* in both the HSC-BMT model (three out of five mice) and the MSC-BMT model (two out of four mice) (Fig. 4*D*). HSC-BMT mice showed better clinical manifestations than untreated *COL17*$^{m-/-}$ mice, whereas mice of the MSC-BMT model had a tendency to show more severe perianal erosions and hair loss (Fig. 4*E*).

Transplanted Human Cord Blood CD34$^+$ Cells Obtain a Keratinocyte-Like Phenotype and Produce Epidermal Component Proteins. Toward clinical applications of stem cell transplantation therapies in human EB patients, we investigated whether the human hematopoietic stem cells have the ability to supply structural proteins in the BMZ of the skin. A human-to-mouse xenogeneic transplantation model was investigated using NOD/SCID/γ_c^{null} (NOG) mice (19). Using immunohistochemistry, human cells that expressed human leukocyte antigen (HLA)-ABC could be seen, and pancytokeratin-positive cells were sporadically costained (0.39 ± 0.15% of the basal cells, $n = 4$) (Fig. 5*A* and *B*), which indicates that these cells are donor cell-derived keratinocytes. In addition, sparse and intermittent hCOL17 was detected along the BMZ in two of seven treated mice (Fig. 5*C*). RT-PCR analysis surprisingly showed mRNA expression of several components of the normal human BMZ other than *hCOL17* (detected in six of seven treated mice), including *BPAG1* (four of seven), *plectin* (four of seven), *α6 integrin* (five of seven), *laminin β3* (two of seven), and *laminin γ2* (one out of seven) (Fig. 5*D*).

Discussion

Junctional EB is caused by mutations in the genes coding for structural proteins anchoring the skin to the underlying basal

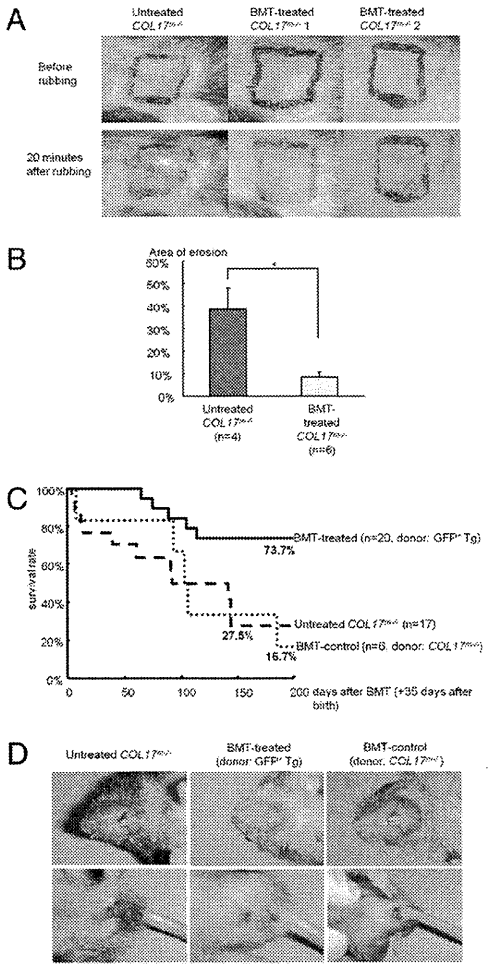

Fig. 3. BMT treatments in $COL17^{m-/-}$ junctional EB model mice change vulnerability to friction in the skin and induce better clinical conditions. (*A*) epithelized areas after erosion formation are investigated by rubber stress test. In untreated $COL17^{m-/-}$ mice, mild mechanical stimulus induces large erosions. Conversely, BMT-treated mice show less severe erosions. $*P < 0.05$. (*B*) The erosion area expressed as a percent of the rubbed area is measured for each group. Resistance of the skin to mechanical stimuli is significantly improved in the BMT-treated $COL17^{m-/-}$ mice. (*C*) Survival curves of BMT-treated and -untreated $COL17^{m-/-}$ mice from d 35 after birth (the day of BMT). $COL17^{m-/-}$ mice treated with BMT from $COL17^{m-/-}$ mice are shown as the BMT control mice; 73.7% of BMT-treated $COL17^{m-/-}$ mice could be expected to live over 200 d after BMT treatment vs. only 27.5% of untreated $COL17^{m-/-}$ mice and 16.7% of BMT control mice. ($P = 0.015$ for BMT-treated vs. untreated mice, $P = 0.021$ for BMT-treated vs. BMT control, and $P = 0.964$ for BMT control vs. untreated.). (*D*) Clinical manifestations at 90 d after BMT treatment (125 d after birth). Untreated $COL17^{m-/-}$ mice show moderate perioral erosions with crusts and anal erosions occurring spontaneously. In contrast, BMT-treated $COL17^{m-/-}$ mice show mild erosions in these areas.

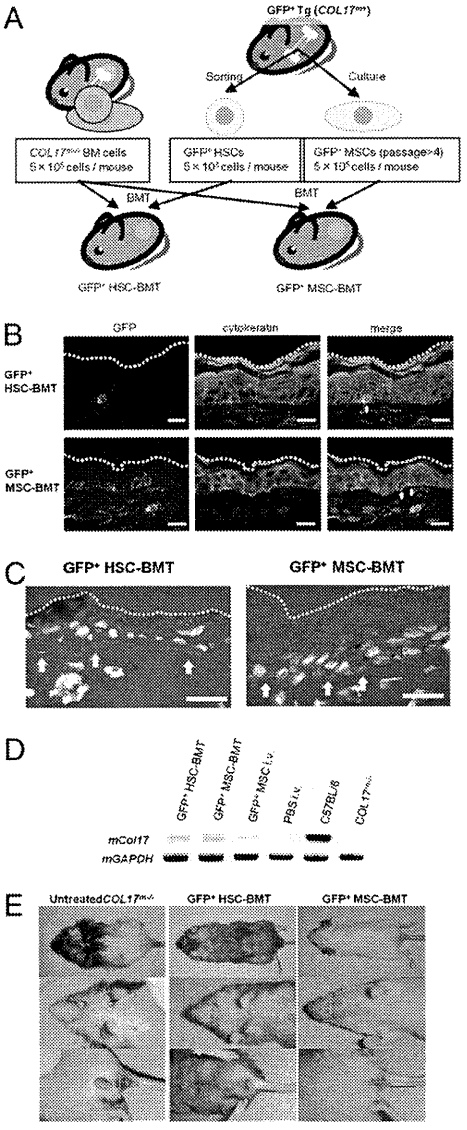

Fig. 4. HSCs and MSCs each have the potential to produce mCol17 in transplanted $COL17^{m-/-}$ mice. (*A*) HSCs and MSCs from GFP^+ Tg mice were sorted or cultured. One or the other type of these stem cells with supporting $COL17^{m-/-}$ whole BM cells were injected into preirradiated $COL17^{m-/-}$ mice. (*B*) Sparse GFP^+ cytokeratin$^+$ cells, shown by white arrows, are detected in the epithelized skin of HSC-BMT model mouse (*Upper*). Also in the MSC-BMT model, GFP^+ cytokeratin$^+$ cells are observed (*Lower*). (Scale bars: 10 μm.) (*C*) Punctate staining of mCol17 is noted, shown as yellow arrows, in the epithelized skin tissue of both HSC- and MSC-BMT model mice. (Scale bars: 20 μm.) (*D*) RT-PCR analysis of the epithelized skin area after full-thickness wounding. Both HSCs (lane 1) and MSCs (lane 2) in the BMT treatment model express positive *mCol17*. Also, single i.v. injection of GFP^+ MSCs (lane 3) induces weak *mCol17* mRNA expression. (*E*) At 90 d after treatment, the HSC-BMT model mice (*Center*) demonstrate better clinical manifestations than the untreated $COL17^{m-/-}$ mice (*Left*), whereas mice of the MSC-BMT models (*Right*) tend to show more severe perianal erosions and hair loss.

lamina and dermis. Recently, various treatments were reported to restore the deficient proteins. These approaches fall mainly into three strategies: gene therapy (20–24), protein therapy (21, 25, 26), and cell therapy. Cell therapies using fibroblasts have been attempted for recessive dystrophic EB (RDEB) model mice and human patients, both of which lack collagen VII. Intradermal fibroblast cell therapy was reported for RDEB model mice (18) and RDEB human patients (27). These approaches may prove to be fundamental treatments for EB. However, their effects are transient and occur only where the genes, proteins, or cells are introduced; they may cause rejection and such gene-correction approaches still raise questions of ethics and safety. Woodley et al. (28) recently reported that i.v. injection of human fibroblasts induces systemic production of human collagen VII in immunodeficient mice; however, major ethical and safety problems remain in human patients.

BMT, an established, widely used medical technique for hematologic malignancies, has recently been attempted for severe hereditary genetic disorders. Hobbs et al. (29) first reported the

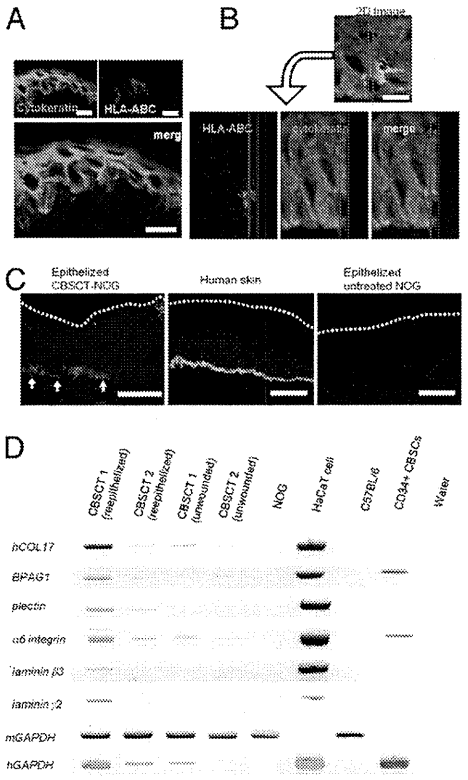

Fig. 5. Human hematopoietic stem cell transplantation induces human epidermal keratinocytes that produce BMZ proteins. (*A*) The epithelized skin samples of treated NOG mice include sporadic cytokeratin$^+$ (red), HLA-ABC$^+$ (blue) cells in the basal cell layer, which indicate human cord blood-derived keratinocytes. (Scale bars: 10 μm.) (*B*) 3D analyses of the immunohistochemical sections prove costaining of keratin (red) and HLA-ABC (green), indicating that these cells are human cord blood-derived keratinocytes and not two distinct overlaid cells. Blue lines: cross-section edges. (Scale bar: 10 μm.) (*C*) Sparse, linear deposition of hCOL17 is noted in the epithelized skin of CBSCT-treated NOG mice (yellow arrows). Green: hCOL17 (D20); red: cytokeratin; (Scale bars: 20 μm.) (*D*) RT-PCR analysis for two transplanted NOG mice, for both unwounded and epithelized skin (CBSCT 1 and CBSCT 2). The expression of several BMZ proteins, *hCOL17, BPAG1, plectin, α6 integrin, laminin β3,* and *laminin γ2* mRNA is demonstrated. Unwounded skin shows faint expression of *hCOL17* and *α6 integrin*.

efficacy of BMT for treatment of Hurler's syndrome. Later hematopoietic stem cell transplantation proved effective in other mucopolysaccharidoses (30–33). More recently, Sampaolesi et al. (34) reported on the potential of stem cell therapy for the treatment of Duchene muscular dystrophy. These experiments indicate that stem cell therapies including BMT are promising candidates for several congenital genetic disorders. BMT techniques have three advantages over previous cell therapies: (*i*) systemic and long-lasting effects can be expected from the circulating BM-derived cells, (*ii*) conventional BMT techniques can be used in clinical applications, and therefore (*iii*) fewer ethical problems arise from the treatment.

Recently Tolar et al. (35) reported that hematopoietic stem cells contributed to life prolongation in RDEB neonatal mice. Chino et al. (36) reported that treatment of embryonic BMT in RDEB mice induced the expression of donor-derived fibroblasts and type VII collagen. These reports investigated neonatal or embryonic mice and focused on type VII collagen, which is produced mainly by dermal fibroblasts. In this study we show the potential of BMT therapies in adult mice with cutaneous congenital disorders caused by deficiencies of transmembrane proteins such as COL17, which is produced mainly by keratinocytes.

As to the origin of the BM-derived cells that differentiated into epidermal cells, Tolar et al. reported that only CD150$^+$ CD48$^-$ HSCs contributed to the amelioration of RDEB mice; nevertheless, MSCs abundantly expressed type VII collagen mRNA (35). Conversely, we and other groups have reported that MSCs also have the potential to differentiate into keratinocytes (37, 38). Our experiments have shown that both HSCs and MSCs have the potential to produce Col17. However, a BMT model with infusion of enriched MSCs tended to induce more severe clinical manifestations. One hypothesis is that the infused MSCs in BMT reside so shortly that long-term effects, such as clinical improvement, might not occur (39, 40). We demonstrated that human cord blood CD34$^+$ HSCs are able to differentiate into keratinocytes in vivo. Although further investigation is needed, we suggest that the difference between the benefits of MSC and HSC transplantations owes to the lack of a long-term, renewable circulating source of Col17-producing cells induced by donor hematopoiesis. From these findings we conclude that both HSCs and MSCs contributed to the production of Col17, although HSCs played more a significant role in clinical improvement in our EB model mice.

Recently Kopp et al. (41) performed BMT and subsequent skin transplantation in one Herlitz-junctional EB infant but unfortunately the child died. They performed normal conditioning treatments similar to those used in hematological malignancies, but the treatments might be too strong for EB patients. Indeed, in our EB model mice, we had to reduce the irradiation dose before BMT to avoid erosions. This report is highly suggestive toward determining conditioning regimens.

In conclusion, we confirmed the reexpression of the previously deficient anchoring protein Col17, better clinical appearance, and longer life expectancy after BMT in our junctional EB model mice. Furthermore we demonstrated that human HSCs can contribute to the regeneration of wounded skin, producing structural proteins in the BMZ. Current conventional hematopoietic stem cell transplantation will lead to treatments for severe forms of EB or even other congenital skin disorders involving epidermal structural proteins.

Materials and Methods

Bone Marrow Transplantation. Recipient adult mice were irradiated with a lethal dose of X-rays at 9 Gy (C57BL/6 and *COL17*$^{m-/-,h+}$ mice) or 6 Gy (in *COL17*$^{m-/-}$ mice), 12 h before infusions. The 9-Gy irradiation resulted in severe erosions and hair loss within 4 wk after BMT to *COL17*$^{m-/-}$ mice. Approximately 3.0–6.0 × 10^6 murine BM-derived cells in 400 μL PBS were injected through the mouse tail vein.

Human Cord Blood Stem Cell Transplantation. Recipient adult NOG mice were irradiated with a sublethal dose of X-rays at 2.5 Gy. Twelve hours later, approximately 1.0–2.5 × 10^5 human CD34$^+$ cells in 400 μL PBS were injected through the mouse tail vein. Hematopoietic reconstitution was evaluated in peripheral blood mononuclear cells 12 wk after transplantation.

Hematopoietic and Mesenchymal Cell Transplantations. Recipient adult *COL17*$^{m-/-}$ mice were irradiated with a lethal dose of X-rays at 6 Gy. Twelve hours later, approximately 5.0 × 10^3 GFP$^+$ HSCs (n = 5) or 5.0 × 10^5 GFP$^+$ MSCs (n = 4) were mixed with 5.0 × 10^5 whole *COL17*$^{m-/-}$ BM-derived cells in 400 μL PBS and injected through the mouse tail vein.

RT-PCR Analyses. For RT-PCR, total RNA from tissues and cells was extracted using Isogen (Nippon Gene) and 200 ng of total RNA was used for cDNA synthesis in SuperScript II reverse transcriptase according to the manufacturer's instructions (Invitrogen). RT-PCR analysis of mRNA was performed in a thermocycler (GeneAmp PCR system 9600; Perkin-Elmer). The primers specific for protein sequences are summarized in Table S1. The PCR protocol for these genes included 35 cycles of amplification (denaturing at 94 °C for 1 min, annealing for 1 min, elongation at 72 °C for 1 min). Aliquots from each amplification reaction were analyzed by electrophoresis in 2% acrylamide-Tris-borate gels. Gel images were acquired and processed by an image analyzer (LAS-4000UVmini; Fujifilm).

Western Blotting. Protein lysates from epidermal tissues were subjected to SDS/PAGE and electrophoretically transferred onto a nitrocellulose membrane. The membranes were blocked with 1% nonfat dry milk in PBS, probed with rat monoclonal antibodies against mCol17 (KT4.2, 1:80,000), and then allowed to react with goat anti-rat IgG antibody coupled with HRP (1:1,000; Southern Biotech). For loading control, we used mouse anti-β-actin antibody

(1:1,000; Sigma-Aldrich) and HRP-conjugated goat anti-mouse IgG (1:1,000; Southern Biotech). The resultant immune complexes were visualized using a chemiluminescent detection system (LumiGLO; Cell Signaling Technology) and processed by an image analyzer (LAS-4000UVmini).

Ultrastructural Observations. Skin biopsy samples of two mice each from GFP$^+$ Tg mice, untreated *COL17*$^{m-/-}$ mice, and BMT-treated *COL17*$^{m-/-}$ mice were fixed in 5% glutaraldehyde solution, postfixed in 1% osmium tetroxide, dehydrated, and embedded in Epon 812. The samples were sectioned at 1-μm thickness for light microscopy and thin-sectioned at 70-nm thickness for electron microscopy. The thin sections were stained with uranyl acetate and lead citrate and examined under a transmission electron microscope (H-7100; Hitachi High-Technologies).

Clinical Evaluation of *COL17*$^{m-/-}$ Mice. After bone marrow transplantation, the clinical severity of the BMT-treated *COL17*$^{m-/-}$ mice, such as spontaneous erosions and blistering, was evaluated and compared with that of the untreated *COL17*$^{m-/-}$ mice and BMT-control mice whose donors were *COL17*$^{m-/-}$ mice. The perioral area and circumanal area tend to be naturally predisposed to erosion. We investigated the clinical severity by measuring the share of each affected area as a percent of its entire region. These were assessed by two independent assessors viewing the same clinical images. In addition we compared the vital prognosis after BMT (35 d after birth) among BMT-treated mice (n = 20), untreated *COL17*$^{m-/-}$ mice (n = 17), and BMT-control mice (n = 6).

Mechanical Rubber Stress Test. The epithelized dorsal skin areas of 1 cm^2 after erosion were marked with a pen and exposed to a mechanical rubber stress test as previously reported (18). The skin was gently stretched, and mechanical shearing forces were applied by the same investigator repeatedly (25 times) as intense, unidirectional rubbing with a pencil eraser. After 20 min, skin specimens were excised and processed for histopathological analysis. Also, we measured the total areas of erosion by ImageJ software (42).

Statistical Analyses. Mann–Whitney U test for nonparametric data, Kaplan-Meier analysis for survival curves, and log-rank test for survival evaluation were performed using Excel 2003 (Microsoft) with the add-in software Statcel2 (OMS) (43). For comparison of more than two groups, data were analyzed by Kruskal–Wallis test followed by Scheffe's F test. Results were expressed as mean ± SE.

ACKNOWLEDGMENTS. We thank Prof. K. B. Yancey (Department of Dermatology, Medical College of Wisconsin, Milwaukee, WI) for providing the *COL17*$^{m+/+,h+}$ mice, Prof. K. Owaribe (Division of Biological Science, Graduate School of Science, Nagoya University, Nagoya, Japan) for the gift of antibodies against human COL17 (D20), and Prof. T. Tanaka (Department of Dermatology, Shiga University of Medical Science, Otsu, Japan) for the gift of antibodies against mouse Col17 (KT4.2). This work was supported in part by grants-in-aid for scientific research (13357008 and 17209038 to H.S. and 15790563 to R.A.) and the Project for Realization of Regenerative Medicine (H.S.) from the Ministry of Education, Science, Sports, and Culture of Japan; by the program for Promotion of Fundamental Studies in Health Sciences of the National Institute of Biomedical Innovation (06-42 to H.S.); by Health and Labor Sciences Research Grants from the Ministry of Health, Labor, and Welfare of Japan (H13-Measures for Intractable Disease-02 and H16-Measures for Intractable Disease-02, to H.S.); and by Japanese Society of Investigative Dermatology (JSID) Fellowship Shiseido Award 2007 (to R.A.).

1. Satake K, Lou J, Lenke LG (2004) Migration of mesenchymal stem cells through cerebrospinal fluid into injured spinal cord tissue. *Spine (Phila Pa 1976)* 29:1971–1979.
2. Herzog EL, Chai L, Krause DS (2003) Plasticity of marrow-derived stem cells. *Blood* 102: 3483–3493.
3. Jiang Y, et al. (2002) Pluripotency of mesenchymal stem cells derived from adult marrow. *Nature* 418:41–49.
4. Orlic D, et al. (2001) Bone marrow cells regenerate infarcted myocardium. *Nature* 410: 701–705.
5. Kocher AA, et al. (2001) Neovascularization of ischemic myocardium by human bone-marrow-derived angioblasts prevents cardiomyocyte apoptosis, reduces remodeling and improves cardiac function. *Nat Med* 7:430–436.
6. Ferrari G, et al. (1998) Muscle regeneration by bone marrow-derived myogenic progenitors. *Science* 279:1528–1530.
7. Yamada M, et al. (2004) Bone marrow-derived progenitor cells are important for lung repair after lipopolysaccharide-induced lung injury. *J Immunol* 172:1266–1272.
8. Kale S, et al. (2003) Bone marrow stem cells contribute to repair of the ischemically injured renal tubule. *J Clin Invest* 112:42–49.
9. Wagers AJ, Sherwood RI, Christensen JL, Weissman IL (2002) Little evidence for developmental plasticity of adult hematopoietic stem cells. *Science* 297:2256–2259.
10. Lagasse E, et al. (2000) Purified hematopoietic stem cells can differentiate into hepatocytes in vivo. *Nat Med* 6:1229–1234.
11. Fine JD, et al. (2008) The classification of inherited epidermolysis bullosa (EB): Report of the Third International Consensus Meeting on Diagnosis and Classification of EB. *J Am Acad Dermatol* 58:931–950.
12. Mavilio F, et al. (2006) Correction of junctional epidermolysis bullosa by transplantation of genetically modified epidermal stem cells. *Nat Med* 12:1397–1402.
13. Banasik MB, McCray PB, Jr (2010) Integrase-defective lentiviral vectors: Progress and applications. *Gene Ther* 17:150–157.
14. Murata H, et al. (2007) Donor-derived cells and human graft-versus-host disease of the skin. *Blood* 109:2663–2665.
15. Harris RG, et al. (2004) Lack of a fusion requirement for development of bone marrow-derived epithelia. *Science* 305:90–93.
16. Inokuma D, et al. (2006) CTACK/CCL27 accelerates skin regeneration via accumulation of bone marrow-derived keratinocytes. *Stem Cells* 24:2810–2816.
17. Nishie W, et al. (2007) Humanization of autoantigen. *Nat Med* 13:378–383.
18. Fritsch A, et al. (2008) A hypomorphic mouse model of dystrophic epidermolysis bullosa reveals mechanisms of disease and response to fibroblast therapy. *J Clin Invest* 118:1669–1679.
19. Ito M, et al. (2002) NOD/SCID/gamma(c)(null) mouse: An excellent recipient mouse model for engraftment of human cells. *Blood* 100:3175–3182.
20. Bauer JW, Lanschuetzer C (2003) Type XVII collagen gene mutations in junctional epidermolysis bullosa and prospects for gene therapy. *Clin Exp Dermatol* 28:53–60.
21. Robbins PB, Sheu SM, Goodnough JB, Khavari PA (2001) Impact of laminin 5 beta3 gene versus protein replacement on gene expression patterns in junctional epidermolysis bullosa. *Hum Gene Ther* 12:1443–1448.
22. Robbins PB, et al. (2001) In vivo restoration of laminin 5 beta 3 expression and function in junctional epidermolysis bullosa. *Proc Natl Acad Sci USA* 98:5193–5198.
23. Dellambra E, et al. (2001) Gene correction of integrin beta4-dependent pyloric atresia-junctional epidermolysis bullosa keratinocytes establishes a role for beta4 tyrosines 1422 and 1440 in hemidesmosome assembly. *J Biol Chem* 276:41336–41342.
24. Seitz CS, Giudice GJ, Balding SD, Marinkovich MP, Khavari PA (1999) BP180 gene delivery in junctional epidermolysis bullosa. *Gene Ther* 6:42–47.
25. Igoucheva O, Kelly A, Uitto J, Alexeev V (2008) Protein therapeutics for junctional epidermolysis bullosa: Incorporation of recombinant beta3 chain into laminin 332 in beta3-/- keratinocytes in vitro. *J Invest Dermatol* 128:1476–1486.
26. Woodley DT, et al. (2004) Injection of recombinant human type VII collagen restores collagen function in dystrophic epidermolysis bullosa. *Nat Med* 10:693–695.
27. Wong T, et al. (2008) Potential of fibroblast cell therapy for recessive dystrophic epidermolysis bullosa. *J Invest Dermatol* 128:2179–2189.
28. Woodley DT, et al. (2007) Intravenously injected human fibroblasts home to skin wounds, deliver type VII collagen, and promote wound healing. *Mol Ther* 15:628–635.
29. Hobbs JR, et al. (1981) Reversal of clinical features of Hurler's disease and biochemical improvement after treatment by bone-marrow transplantation. *Lancet* 2:709–712.
30. Sands MS, et al. (1997) Murine mucopolysaccharidosis type VII: Long term therapeutic effects of enzyme replacement and enzyme replacement followed by bone marrow transplantation. *J Clin Invest* 99:1596–1605.
31. Warkentin PI, Dixon MS, Jr, Schafer I, Strandjord SE, Coccia PF (1986) Bone marrow transplantation in Hunter syndrome: A preliminary report. *Birth Defects Orig Artic Ser* 22:31–39.
32. Krivit W, et al. (1984) Bone-marrow transplantation in the Maroteaux-Lamy syndrome (mucopolysaccharidosis type VI). Biochemical and clinical status 24 months after transplantation. *N Engl J Med* 311:1606–1611.
33. Gasper PW, et al. (1984) Correction of feline arylsulphatase B deficiency (mucopolysaccharidosis VI) by bone marrow transplantation. *Nature* 312:467–469.
34. Sampaolesi M, et al. (2006) Mesoangioblast stem cells ameliorate muscle function in dystrophic dogs. *Nature* 444:574–579.
35. Tolar J, et al. (2009) Amelioration of epidermolysis bullosa by transfer of wild-type bone marrow cells. *Blood* 113:1167–1174.
36. Chino T, et al. (2008) Bone marrow cell transfer into fetal circulation can ameliorate genetic skin diseases by providing fibroblasts to the skin and inducing immune tolerance. *Am J Pathol* 173:803–814.
37. Wu Y, Chen L, Scott PG, Tredget EE (2007) Mesenchymal stem cells enhance wound healing through differentiation and angiogenesis. *Stem Cells* 25:2648–2659.
38. Sasaki M, et al. (2008) Mesenchymal stem cells are recruited into wounded skin and contribute to wound repair by transdifferentiation into multiple skin cell type. *J Immunol* 180:2581–2587.
39. Rieger K, et al. (2005) Mesenchymal stem cells remain of host origin even a long time after allogeneic peripheral blood stem cell or bone marrow transplantation. *Exp Hematol* 33:605–611.
40. Dickhut A, et al. (2005) Mesenchymal stem cells obtained after bone marrow transplantation or peripheral blood stem cell transplantation originate from host tissue. *Ann Hematol* 84:722–727.
41. Kopp J, et al. (2005) Hematopoietic stem cell transplantation and subsequent 80% skin exchange by grafts from the same donor in a patient with Herlitz disease. *Transplantation* 79:255–256.
42. Abramoff MD, Magelhaes PJ, Ram SJ (2004) Image Processing with ImageJ. *Biophotonics International* 11:36–42.
43. Yanai H (2004) *Statcel-The Useful Add-In Software Forms on Excel* (OMS, Tokyo) 2nd Ed.

Corrections and Retraction

CORRECTIONS

GENETICS

Correction for "Lack of association of common variants on chromosome 2p with primary open-angle glaucoma in the Japanese population," by Fumihiko Mabuchi, Yoichi Sakurada, Kenji Kashiwagi, Zentaro Yamagata, Hiroyuki lijima, and Shigeo Tsukahara, which appeared in issue 21, May 25, 2010, of *Proc Natl Acad Sci USA* (107:E90–E91; first published April 27, 2010; 10.1073/pnas.0914903107).

The authors note that, due to a printer's error, the author name Hiroyuki lijima should have appeared as Hiroyuki Iijima. The corrected author line appears below. The online version has been corrected.

Fumihiko Mabuchi[a,1], Yoichi Sakurada[a], Kenji Kashiwagi[a], Zentaro Yamagata[b], Hiroyuki Iijima[a], and Shigeo Tsukahara[a]

www.pnas.org/cgi/doi/10.1073/pnas.1008743107

MEDICAL SCIENCES

Correction for "Bone marrow transplantation restores epidermal basement membrane protein expression and rescues epidermolysis bullosa model mice," by Yasuyuki Fujita, Riichiro Abe, Daisuke Inokuma, Mikako Sasaki, Daichi Hoshina, Ken Natsuga, Wataru Nishie, James R. McMillan, Hideki Nakamura, Tadamichi Shimizu, Masashi Akiyama, Daisuke Sawamura, and Hiroshi Shimizu, which appeared in issue 32, August 10, 2010, of *Proc Natl Acad Sci USA* (107:14345–14350; first published July 26, 2010; 10.1073/pnas.1000044107).

The authors note that, due to a printer's error, Yasuyuki Fujita was omitted as the first author of this article. The corrected author line appears below. The online and print versions have been corrected.

Yasuyuki Fujita[a], Riichiro Abe[a,1], Daisuke Inokuma[a], Mikako Sasaki[a], Daichi Hoshina[a], Ken Natsuga[a], Wataru Nishie[a], James R. McMillan[a], Hideki Nakamura[a], Tadamichi Shimizu[b], Masashi Akiyama[a], Daisuke Sawamura[c], and Hiroshi Shimizu[a,1]

www.pnas.org/cgi/doi/10.1073/pnas.1011158107

RETRACTION

MEDICAL SCIENCES

Retraction for "Complete and persistent phenotypic correction of phenylketonuria in mice by site-specific genome integration of murine phenylalanine hydroxylase cDNA," by Li Chen and Savio L. C. Woo, which appeared in issue 43, October 25, 2005, of *Proc Natl Acad Sci USA* (102:15581–15586; first published October 17, 2005; 10.1073/pnas.0503877102).

The undersigned author wishes to note the following: "After re-examining the laboratory records, I have concluded that there are data irregularities underlying this paper that warrant its retraction. I regret not recognizing these irregularities before the manuscript was published and apologize for any inconvenience this might have caused."

Savio L. C. Woo

www.pnas.org/cgi/doi/10.1073/pnas.1009071107

the FEBS Journal

Identification of a preferred substrate peptide for transglutaminase 3 and detection of *in situ* activity in skin and hair follicles

Asaka Yamane[1,*], Mina Fukui[1,*], Yoshiaki Sugimura[1], Miho Itoh[1], Mileidys Perez Alea[2], Vincent Thomas[2], Said El Alaoui[2], Masashi Akiyama[3] and Kiyotaka Hitomi[1]

1 Department of Applied Molecular Biosciences, Graduate School of Bioagricultural Sciences, Nagoya University, Japan
2 CovalAb, Villeurbanne, France
3 Department of Dermatology, Hokkaido University Graduate School of Medicine, Sapporo, Japan

Keywords
epidermis; hair follicle; phage-display; skin; transglutaminase

Correspondence
K. Hitomi, Department of Applied Molecular Biosciences, Graduate School of Bioagricultural Sciences, Nagoya University, Nagoya 464-8601, Japan
Fax: +81 52 789 5542
Tel: +81 52 789 5541
E-mail: hitomi@agr.nagoya-u.ac.jp

*These authors contributed equally to this work

(Received 13 May 2010, revised 4 July 2010, accepted 6 July 2010)

doi:10.1111/j.1742-4658.2010.07765.x

Transglutaminases (TGases) are a family of enzymes that catalyze cross-linking reactions between proteins. During epidermal differentiation, these enzymatic reactions are essential for formation of the cornified envelope, which consists of cross-linked structural proteins. Two main transglutaminases isoforms, epidermal-type (TGase 3) and keratinocyte-type (TGase 1), are cooperatively involved in this process of differentiating keratinocytes. Information regarding their substrate preference is of great importance to determine the functional role of these isozymes and clarify their possible co-operative action. Thus far, we have identified highly reactive peptide sequences specifically recognized by TGases isozymes such as TGase 1, TGase 2 (tissue-type isozyme) and the blood coagulation isozyme, Factor XIII. In this study, several substrate peptide sequences for human TGase 3 were screened from a phage-displayed peptide library. The preferred substrate sequences for TGase 3 were selected and evaluated as fusion proteins with mutated glutathione *S*-transferase. From these studies, a highly reactive and isozyme-specific sequence (E51) was identified. Furthermore, this sequence was found to be a prominent substrate in the peptide form and was suitable for detection of *in situ* TGase 3 activity in the mouse epidermis. TGase 3 enzymatic activity was detected in the layers of differentiating keratinocytes and hair follicles with patterns distinct from those of TGase 1. Our findings provide new information on the specific distribution of TGase 3 and constitute a useful tool to clarify its functional role in the epidermis.

Introduction

Transglutaminases (TGases: EC 2.3.2.13) are a family of enzymes that catalyze the calcium-dependent formation of isopeptide cross-links between glutamine and lysine residues in various proteins [1,2]. Furthermore, these enzymatic reactions include the attachment of primary amines to peptide-bound glutamine residues, and the conversion of glutamine to glutamic acid. To date, eight TGase isozymes (Factor XIII, TGases 1–7),

Abbreviations
bio-Cd, 5-(biotinamido)pentylamine; CE, cornified envelope; Dansyl-Cd, monodansylpentylamine; FITC, fluorescein isothiocyanate; GST, glutathione *S*-transferase; SPR, small proline-rich protein; TBS, Tris/buffered saline; TGase, transglutaminase.

comprising a protein family with unique substrate specificities and different tissue distributions, have been identified in mammals. Factor XIII and TGase 2 are involved in the stabilization of fibrin clots and various roles including apoptosis, extracellular matrix formation and wound healing, respectively [3–6]. TGase 1 and TGase 3 have been reported to contribute to the formation of the epidermis by cross-linking structural proteins in keratinocytes [7–9]. TGase 4 is expressed in the prostate and is reported to be involved in plug formation in rodents [10]. The biochemical characterization and physiological roles of TGase 5 (expressed in keratinocytes), TGase 6 and TGase 7 remain unknown [11,12].

In a TGase-catalyzed reaction, a glutamine residue in the substrate binds to the cysteine residue at the active site of the enzyme, resulting in the formation of an intermediate. This is a rate-limiting step because not all glutamine residues participate in the reaction. By contrast, the reaction with the second substrate, a lysine residue or a primary amine, is less selective. Moreover, distinct isozymes recognize distinct glutamine residues in the same protein. Therefore, primary and secondary structures surrounding the reactive glutamine residues are critical in the formation of an intermediate enzyme–substrate complex. Each isozyme in the TGase family, mainly characterized as TGase 1, TGase 2 and Factor XIII, demonstrates different substrate recognition patterns because the glutamine residues in the substrate involved in binding to the enzyme are isozyme specific [13,14].

We have established a screening system that employs a phage-displayed random peptide library to characterize the preferred substrate sequences for TGase [15–18]. In a series of studies, 12-mer sequences acting as isozyme-specific substrates for Factor XIII, TGase 1 and TGase 2 were obtained. From these studies, we selected the most reactive and isozyme-specific substrate sequences that were functional not only as phage-display proteins, but also as peptide forms. Furthermore, in our recent reports, the most reactive peptide sequence (K5), selected as a TGase 1-preferred substrate, was successfully used as a probe to detect *in situ* enzymatic activity in both human and mouse skin [16,19]. These studies have provided new insight into the substrate specificity of Tgases and have expanded the range of application of the enzyme reaction [20].

TGase 3, initially designated as an epidermal-type enzyme, is responsible for formation of the epidermis [21,22]. In the current model of TGase function, during keratinocyte differentiation, TGase 1 and TGase 3 are believed to act cooperatively in the cross-linking of proteins, including involucrin, loricrin and small proline-rich proteins (SPRs). Such concerted reactions result in formation of the cornified envelope (CE), a specialized component consisting of covalent cross-links of proteins beneath the plasma membrane of terminally differentiated keratinocytes [23,24]. Furthermore, TGase 3 in hair follicles is involved in cross-linking structural proteins such as trichohyalin and keratin intermediate to hardening the inner root sheath. In this case, TGase 1 co-operates with TGase 3 through a cross-linking reaction to produce stable hair fibers.

During differentiation in these processes, a zymogen form of TGase 3 (77 kDa) is activated by limited proteolysis with cathepsins S and/or L [25,26]. Although several studies have focused on the localization, structural analysis and activation mechanism of TGase 3 zymogen, not much information is available about the substrate specificity and physiological function of the active form [27–31]. In particularly, the precise substrate specificity and local activation areas of TGase 1 and TGase 3 in the epidermis have not been fully identified.

In this study, we applied a screening system to obtain the preferred substrate peptides for human TGase 3. The selected phages displayed a unique tendency toward the primary sequences, and the most reactive and isozyme-specific sequence among the peptide sequences was determined. Furthermore, this sequence proved to be a prominent substrate in the peptide form. Specific localization of activated TGase 3, which was found to display a pattern distinct from that of TGase 1, was observed by the detection of *in situ* activities using this peptide.

Results

Screening of candidate substrate sequences from a random peptide library

Phage clones in a random peptide library were incubated with biotinylated cadaverine (bio-Cd), a glutamine-acceptor substrate, in the presence of the activated form of human TGase 3 (Fig. S1). By the enzymatic reaction, phage particles displaying the reactive glutamine residues preferably incorporate bio-Cd. Avidin affinity purification resulted in the selection of phage particles that covalently bound bio-Cd. The phage particles were amplified and subjected to four additional enzymatic reactions and panning. Sequence analysis of the finally selected individual phage clones (125 clones) revealed that $\sim$ 93.6% (117/125) of the clones displayed peptide sequences containing glutamine residue. In this process, false-positive clones containing no glutamine residue might be co-purified if the sequence has an affinity to avidin.

When the peptide sequences were aligned and analyzed with respect to the potential reactive glutamine residue, the following significant tendencies among the sequences were observed: (a) a hydrophobic amino acid was commonly observed at position +3 (relative to the glutamine residue); (b) lysine or arginine mainly was found at position +2; and (c) in most sequences, an aromatic amino acid and a serine/threonine residue were frequently located at positions −1 and +1, respectively. Figure 1 shows the representative sequences that were further analyzed for their reactivity as substrates.

Evaluation of selected sequences as recombinant peptide-fused glutathione *S*-transferase (GST) proteins

To evaluate the ability of the screened peptide sequences as a glutamine-donor substrate, we measured the amount of enzymatic incorporation of the primary amine, monodansylcadaverine (Dansyl-Cd), in recombinant peptide-GST(QN) fusion proteins, in which all the glutamine residues in glutathione *S*-transferase (GST) had been substituted by asparagines. The peptide sequences shown in Fig. 1 were expressed as

*E12			Y	D	Y	W	P	M	Q	T	R	T	R	T					
*E50					W	G	P	Q	Q	T	R	I	P	S	Y	R			
E524				I	K	F	P	E	Q	T	R	I	W	H	A				
*E8							W	T	Q	T	R	F	T	T	P	F	P	E	
E47					E	W	F	G	Q	V	R	I	H	P	M	S			
*E51		P	P	P	Y	S	F	Y	Q	S	R	W	V						
*E10				W	N	F	A	E	Q	T	R	L	F	K	A				
*E21						L	M	P	Q	T	R	L	E	P	H	M	L		
E33								F	Q	M	R	L	P	L	A	G	P	S	F
E9								Y	Q	Q	R	L	Y	M	P	T	W	P	P
*E1								Y	Q	T	K	W	P	M	E	F	S	S	R
*E18								F	Q	L	K	V	P	A	A	V	W	S	D
*E6								Y	Q	L	K	Y	T	H	W	A	H	T	P
E53								F	Q	Y	K	L	N	F	G	Q	Y	V	Y
*E125	A	E	R	P		N	I	M	Q	V	K	L	V						
*E42						W	T	T	Q	M	K	M	P	H	H	A	F		
E110							F	Y	Q	R	P	L	P	A	H	L	L	G	
*E4						F	N	Y	Q	A	Y	L	D	I	P	R	Y		
E55						F	P	Y	Q	T	L	F	N	P	T	P	M		
E68						W	P	Y	Q	I	M	M	G	H	A	R	A		
*E46	N	Y	W	S		W	P	G	Q	I	S	Y	H						
E17						N	P	Y	Q	Y	Q	I	F	N	W	A	W		
E510						W	E	T	Q	Q	S	W	L	F	S	N	L		
E45							T	Y	Q	H	I	W	H	P	S	L	A	L	
E5								Y	Q	I	T	L	P	Y	R	Y	E	M	P
*E111								W	Q	S	P	I	T	F	P	L	T	L	A
*E115								W	Q	T	Q	V	V	L	H	E	E	P	L
E70							Y	S	Q	S	T	H	A	L	F	S	A	R	
*E2					K	M	P	E	D	T	R	L	H	N	F	A			

Fig. 1. Selected sequences and alignment of candidate substrate peptide. Selected 12-mer peptide sequences were aligned based on the putative reactive glutamine residue. The glutamine residue, hydrophobic amino acids at position +3 (relative to the glutamine), and the arginine and the lysine residues at position +2 are shaded. Phage ID (E) is shown at the left of the amino acid sequence. The asterisk indicates the sequences of which reactivities were subsequently shown in Fig. 2.

fusion proteins and the time-course products formed by the catalytic reaction of TGase 3 were subjected to SDS/PAGE and visualized by UV illumination. Using this procedure, 16 of the 29 sequences, including a no-glutamine-containing sequence as a negative control, were selected based on their reactivities (Fig. 1, marked with asterisk). The enzymatic products, with dimethylcasein as a positive control, were aligned as shown in Fig. 2A. Among the sequences that exhibited incorporation of Dansyl-Cd, seven peptides (underlined sequences: E8, E12, E18, E115, E46, E10 and E51) were selected based on their reactivities and further analyzed for their isozyme specificity with respect to human TGase 1, guinea-pig liver TGase (as TGase 2) and human Factor XIII (Fig. 2B). All the sequences showed negligible reactivity in the reaction catalyzed by Factor XIII. However, five sequences (E8, E12, E115, E46 and E10) exhibited cross-reactivities to guinea-pig liver TGase and one (E18) to TGase 1. Among the seven peptide–GST(QN) fusion proteins evaluated in this study, only the E51 sequence showed less cross-reactivity to other isozymes although displaying prominent reactivity to TGase 3. Thus, this peptide sequence was selected for further analysis.

Substitution-mutant analysis for each amino acid to alanine in the E51 peptide sequence

To examine the contribution of each amino acid residue of the E51 sequence (PPPYSFYQSRWV) in the catalytic reaction of TGase 3, alanine substitution mutants for every residue of the 12-amino acid peptide were generated as GST(QN)-fusion proteins. Wild-type and a mutant in which the reactive glutamine was substituted by asparagine were also subjected to the analysis (Fig. 3). According to the catalytic reaction of TGase 3, substitutions at positions −2 (F), +1 (S), +2 (R) and +3 (W) significantly affected the reactivity (colored as darker gray: < 50% intensity of that in wild-type). In addition, substitution at positions −5 (P) and +4 (V) resulted in a moderate decrease in reactivity. These results suggest that these amino acids contribute to the interaction of E51 with the enzyme to form an intermediate between the glutamine residue in the substrate and the cysteine residue in the active site pocket of TGase 3.

Assessment of reactivity and specificity of E51 sequence in the peptide form (pepE51)

To assess the reactivity and isozyme-specificity of E51 (PPPYSFYQSRWV) in peptide form, biotinylated peptides for E51 (pepE51) or E51 in which the reactive

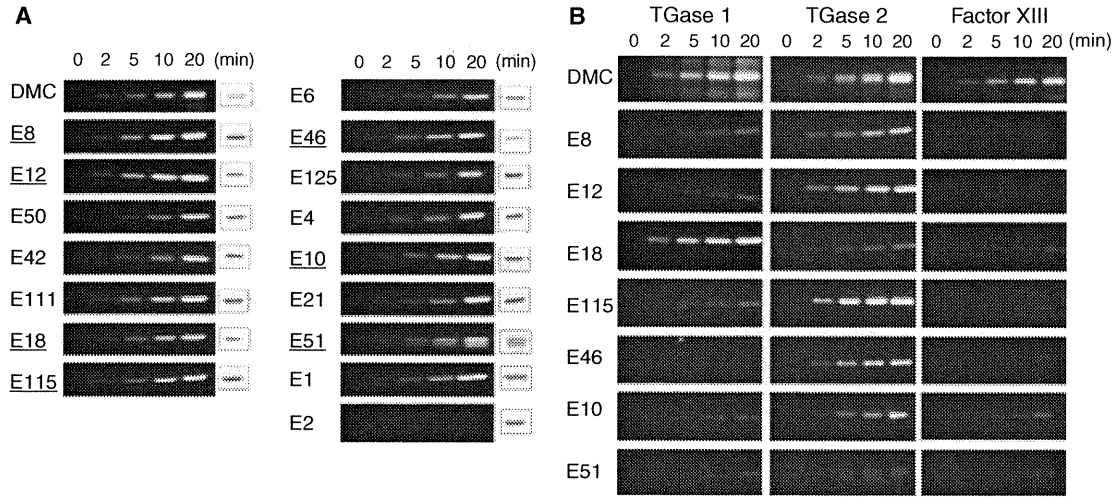

Fig. 2. Evaluation of the reactivities of the selected peptides as GST(QN) fusion proteins. (A) Incorporation of Dansyl-Cd into the purified recombinant GST(QN) fusion proteins with peptide that were selected by phage display screening, in the presence of activated TGase 3 (1 ng·μL^{-1}). At the times indicated, the reaction products were separated on 12.5% SDS/PAGE and illuminated by UV light. Unreacted fusion proteins were stained with Coomassie Brilliant Blue and are shown on the right. The underlined sequences are subjected to further analysis for cross-reactivities. (B) Cross-reactivities to three isozymes regarding the selected seven GST(QN)-fusion proteins. Each protein reacted at the indicated times in the presence of TGase 1 (1.5 ng·μL^{-1}), guinea-pig liver TGase (TGase 2) (2.5 ng·μL^{-1}) and activated Factor XIII (5 ng·μL^{-1}) were analyzed by SDS/PAGE and UV illumination. All the enzymatic activities were normalized based on the incorporation of Dansyl-Cd into dimethylcasein.

glutamine residue was substituted by asparagine (pepE51QN: PPPYSFYNSRWV) were synthesized for examination. Both peptides were subjected to a TGase 3-catalyzed cross-reaction with a primary amine (spermine), covalently immobilized to a microtiter well, in the presence of activated TGase 3 [32,33]. As shown in Fig. 4A, a time-course-dependent incorporation of pepE51 was observed, whereas pepE51QN did not show any reactivity. Moreover, in contrast to pepE51QN, increasing concentrations of pepE51 enzymatically cross-linked with the coated spermine (Fig. 4B). In addition, β-casein as a glutamine-acceptor substrate appeared to accept pepE51 (data not shown). These results demonstrate that pepE51 acts as a good substrate, similarly to the fusion protein.

To further investigate whether the isozyme specificity was preserved, the reactivity of pepE51 at various concentrations was evaluated in the presence of other TGase isozymes including TGase 1, TGase 2 and activated Factor XIII (Fig. 5). A negative control was paralleled using pepE51QN. In each case, pepE51 showed less cross-reactivity with the isozymes at the examined peptide concentrations, except for a weak reaction with guinea-pig liver TGase at a higher concentration (> 2.5 μM). This result suggests that pepE51 at a concentration below 1 μM can be used as a specific peptide in this reaction.

Detection of *in situ* activities of TGase in the skin and hair follicles

Previously, we found that a fluorescent-labeled substrate peptide for TGase 1 [fluorescein isothiocyanate (FITC)–pepK5] could be used as a prominent probe for detecting *in situ* activity of TGase 1 in both mouse and human skin [16,19]. Therefore, using a similar procedure, fluorescent-labeled E51 peptide (FITC–pepE51) was prepared and evaluated for detecting *in situ* activity of TGase 3 in a frozen mouse skin section.

As shown in Fig. 6, in the presence of $CaCl_2$, specific incorporation of FITC–pepE51 (1 μM) in endogenous glutamine-acceptor substrate proteins was observed in the epidermis. Reaction using FITC–pepE51QN, or in the presence of EDTA resulted in no signal, indicating that the signal was specific for TGase 3 activity.

Moreover, we inspected enlarged images of the skin section (Fig. 7A). In the epidermis, positive signals were observed around the granular and spinous layers and not in the outermost cornified layers, judging from the merged image with differential interference images. When compared with signals obtained using FITC–pepK5, the slightly weak and more limited regions in the layers were stained with FITC–pepE51. This result suggested that TGase 3 was active in more differentiating keratinocytes.

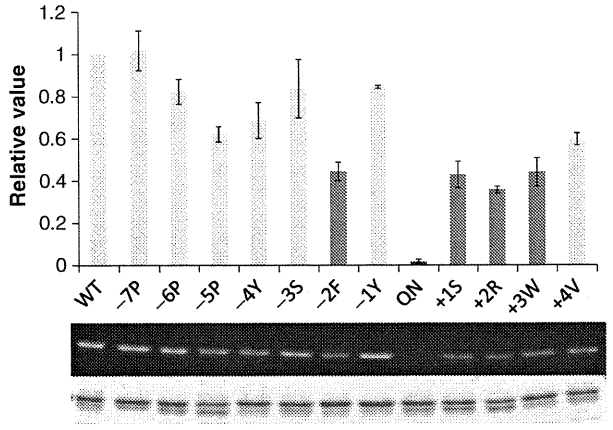

Fig. 3. Assessment of contribution of each amino acid residue of E51 sequence to substrate recognition. Alanine substitution mutants in the E51 sequence were produced as GST(QN) fusion proteins, and then incubated with Dansyl-Cd for 10 min in the presence of activated TGase 3 (1 ng·μL^{-1}). The reaction products were subjected to SDS/PAGE, followed by UV illumination. The fluorescence intensity was analyzed by Fuji multigauge quantification system. The relative values are normalized to the intensity for the reaction of wild-type. Data represent the means ± SD of duplicate samples. Numbers (−7P to +4V) with amino acid residue indicate the position of substitution; WT, peptide in which there were no amino acid substitution; QN, peptide in which the glutamine residue was changed to asparagine. The mutations that resulted in decrease in the reactivity at < 50% of that in wild type are shaded in darker gray.

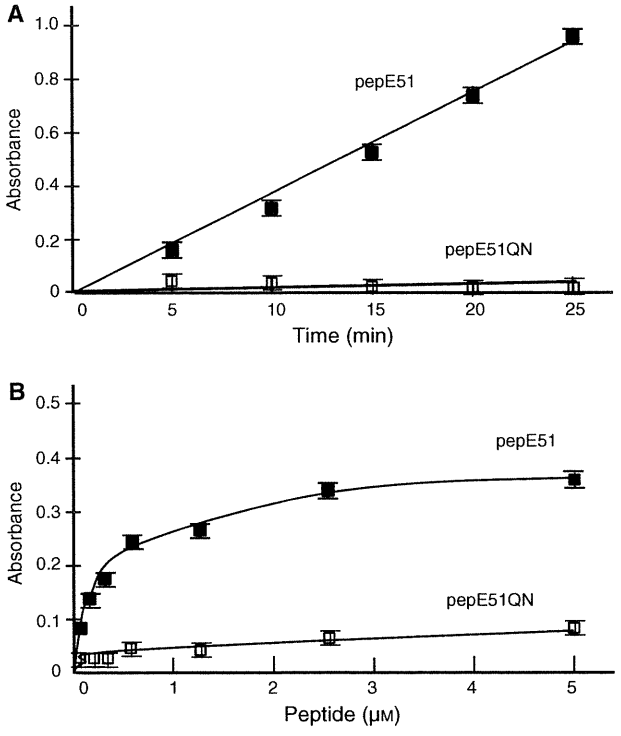

Fig. 4. Analysis of the reactivity of E51 sequence in the peptide form. (A) The time-dependent incorporation of 5 μM biotinylated peptide E51 (pepE51) into spermine, that covalently attached to microtiter well, was examined in the presence of activated TGase 3 (0.5 ng·μL^{-1}). The mutant peptide in which the glutamine was changed to asparagine (pepE51QN) was paralleled. (B) On the various concentrations of biotin-labeled peptides, incorporation into coated-spermine was measured in the same reaction condition at incubation time of 10 min. The closed and open symbols represent the reactions for pepE51 and pepE51QN, respectively. Data represent the means ± SD of triplicate samples.

Next, the staining pattern of the hair follicles was investigated (Fig. 7B,C). The distribution of signals was different when FITC–pepK5 and FITC–pepE51 were used. According to the FITC–pepE51 pattern, the activated TGase 3 was mainly located in the medulla and the hair cortex. However, according to the FITC–pepK5 pattern, TGase 1 activity was observed around the outer root sheath and cuticle and in differentiated inner root sheath cells. Thus, TGase 1 and TGase 3 appeared active in distinct regions of the hair follicle cells.

Discussion

During differentiation of keratinocytes and hair formation, isopeptide cross-linking of several structural proteins is essential for the formation of the insoluble proteinaceous layers, the CE, which contribute to effective physical and water barrier formation. Upon CE formation in keratinocytes and hair follicle cells, TGase 3 cross-links various substrate proteins such as SPRs, involucrin, loricrin and trichohyalin [7–9,23,24]. In addition to the endogenous substrates, some proteins of human papillomavirus have been described as possible substrates for inducing an abnormality in CE formation [34]. Previous studies have determined the cross-linking sites of these proteins and suggest that they display a pattern distinct from that obtained with TGase 1 [35–38]. In these reports, for example, the sequences QLQQQQVK (SPR1, Q19), SQQVTQT (loricrin, Q219), HQTQQK (loricrin, Q305), SSQQQKQ (SPR1, Q5 and Q7) and SQQVTQT (loricrin, Q215 and Q216) were determined as cross-linking sites by TGase 1 and TGase 3, respectively. However, differences in reaction specificities between these two isozymes are not fully understood. A better understanding of the preferred substrate sequences for TGase 3 will provide useful information for clarifying the process of cross-linking.

To date, with respect to the major members of the TGases family such as TGase 1, TGase 2 and Factor XIII, we have investigated the preferred substrate

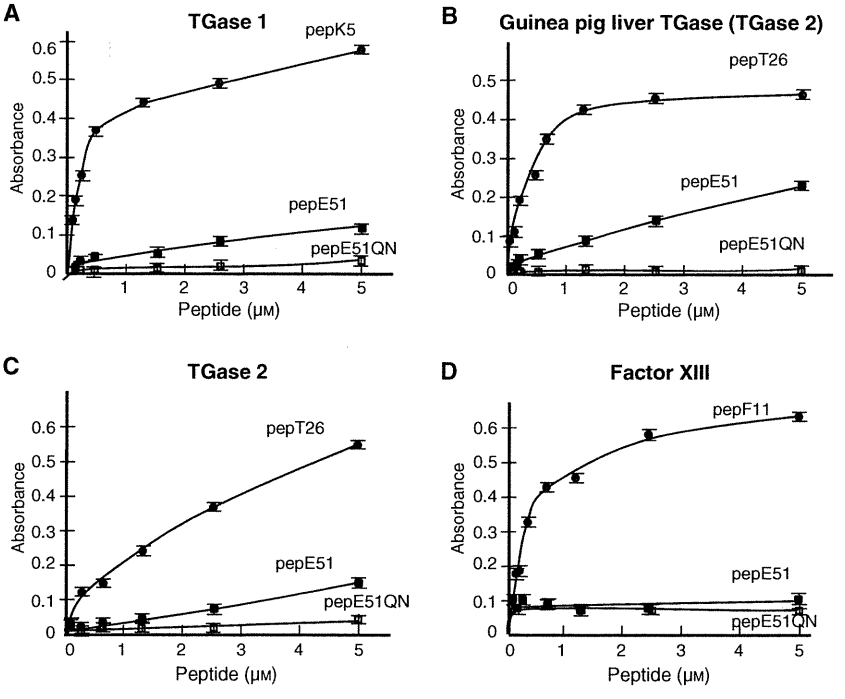

Fig. 5. Cross-reactivities of pepE51 with other major isozymes. On the various concentrations of pepE51 and pepE51QN as well as three specific biotin-labeled peptides (pepK5; TGase 1, pepT26; TGase 2, pepF11; Factor XIII), incorporation into coated-spermine was measured in the presence of each isozyme, TGase 1 (0.075 ng·μL^{-1}) (A), guinea-pig liver TGase (0.12 ng·μL^{-1}) (B), TGase 2 (0.06 ng·μL^{-1}) (C), and activated Factor XIII (0.24 ng·μL^{-1}) (D) for 15 min. All the enzymatic activities were normalized based on the incorporation of Dansyl-Cd into dimethylcasein. The closed circles represent the reactions for pepK5, pepT26 and pepF11 in each isozyme reaction. The closed and open rectangles indicate the reaction for pepE51 and pepE51QN, respectively. Data represent the means ± SD of triplicate samples.

sequences around the reactive glutamine residue from a phage-displayed peptide library [15,16]. In these previous studies, the identified preferred substrate sequences displayed a unique tendency for each isozyme, Q-x-R/K-Ψ-x-x-x-W-P to TGase 1, Q-x-P-Ψ-D-P to TGase 2 and Q-x-x-Ψ-x-W-P to Factor XIII (x and Ψ are any amino acid and hydrophobic amino acid residues, respectively). We applied a similar approach to obtain information regarding the preferred substrate sequence for TGase 3, with particular interest in a highly reactive substrate peptide suitable for the detection of *in situ* enzymatic activity.

In this study, the preferred sequences for TGase 3 selected from the phage-displayed peptide library exhibited different tendencies compared with other TGase isozymes. With respect to the peptides that exhibited higher reactivities to TGase 3, the Q-S/T-K/R-Ψ consensus primary sequence was identified. The sequence motif, Q-x-K/R is frequently observed in several skin substrate sequences and also contained in the preferred substrate sequence that we previously identified for TGase 1 [16]. In the case of TGase 3, serine or threonine residues are frequently observed at position +1. Interestingly, the amino acid located at this position is not important for the reaction in other Tgases, including TGase 1. In addition, at the N-terminal side of the glutamine residue including position -1, bulk amino acid residues such as tyrosine, proline and phenylalanine are located in the case of the selected sequence for TGase 3. This tendency is specific to TGase 3 and is not observed in TGase 1 and other isozymes.

Among the selected sequences, E51 (PPPYS-FYQSRWV) was the most prominent substrate with respect to TGase 3 reactivity and isozyme specificity. This sequence also satisfied the amino acid residue tendency, described previously. Alanine substitutions at positions −2, +1, +2 and +3 of the selected E51 sequence significantly affected reactivity. The results suggest that these residues are essential for interaction with activated TGase 3.

Recently, we established a rapid and sensitive assay system using biotinylated preferred substrate peptide and spermine-coated microtiter plates. The reactivity and specificity of the E51 sequence was maintained in a biotinylated peptide form (pepE51) when the primary amine was used as a glutamine-acceptor substrate. At low concentrations, pepE51 exhibits high reactivity with TG3 and very low reactivity with other isozymes under these enzymatic activities (Fig. 5). In the case of guinea-pig liver TGase, used as TGase 2, a weak cross-reactivity was observed possibly resulting from the co-purification of activated TGase 3. Thus, the synthesized peptide for the E51 sequence represents a valuable tool for studying TGase 3 substrate recognition and enzymatic activity.

Therefore, we examined the ability of the E51 sequence to detect endogenous TGase activity in the

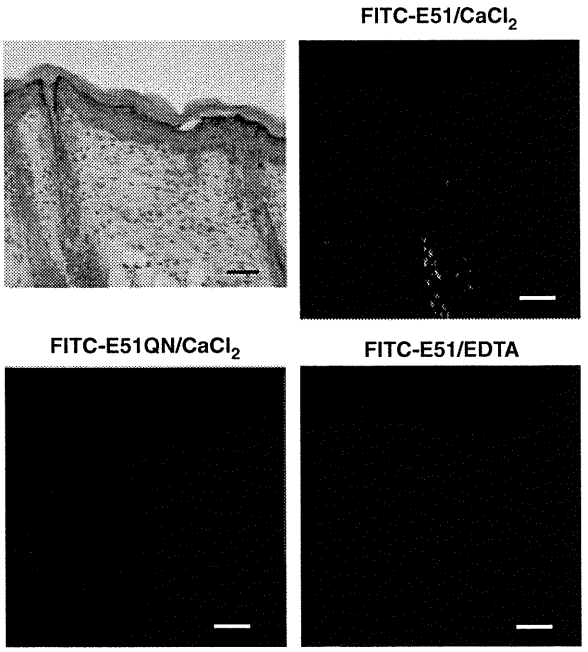

Fig. 6. Detection of *in situ* TGase 3 activities in the mouse skin section. Hematoxylin and eosin staining is shown at the left. FITC–pepE51 (1 μM) was reacted with frozen mouse skin section in the presence of $CaCl_2$. As a negative control, incubation with FITC–pepE51QN and co-presence of EDTA in the reaction of pepE51 were carried out under the same reaction condition. Bar represents 50 μm.

skin, as previously established for TGase 1-preferred substrate peptide, K5 [16]. Using a similar approach, calcium-dependent incorporation of FITC–pepE51 through its glutamine residue into lysine residues of endogenous substrate proteins was observed (Figs 6 and 7). TGase 3 has been observed in both differentiating keratinocytes and hair follicles of the epidermis by immunochemical analyses [38–40]. However, in this study, we present the first direct evidence for the detection of activated TGase 3 in the epidermis. Therefore, this finding provides more precise information on the physiological significance of TGase 3 because this enzyme is synthesized as an inactive zymogen form.

In the epidermis, endogenous TGase 3 activity was observed mostly in the granular and spinous layers. However, the activity was detected within a more limited region when compared with the staining results obtained with FITC–pepK5, a preferred substrate for TGase 1. In addition, in hair follicle cells, the staining pattern of TGase 3 was distinct from that of TGase 1. *In situ* activity of the enzyme was observed mainly around the inner root sheath, which is consistent with results obtained previously using immunostaining analyses [39,40]. By contrast, TGase 3 activity was found around the medulla and hair cortex. These results for TGase 3 in the epidermis and hair follicles are convincing; however, in cells with higher TGase 1 activity, there might be the possibility of a slight cross-reaction with TGase 1.

In a recent study that used immunochemical analysis and *in situ* detection of the activity by FITC-labeled cadaverine, Thibaut *et al.* [40] reported that TGase 3 was mainly present in hair fibers. This is mostly consistent with our results. However, in their study, the

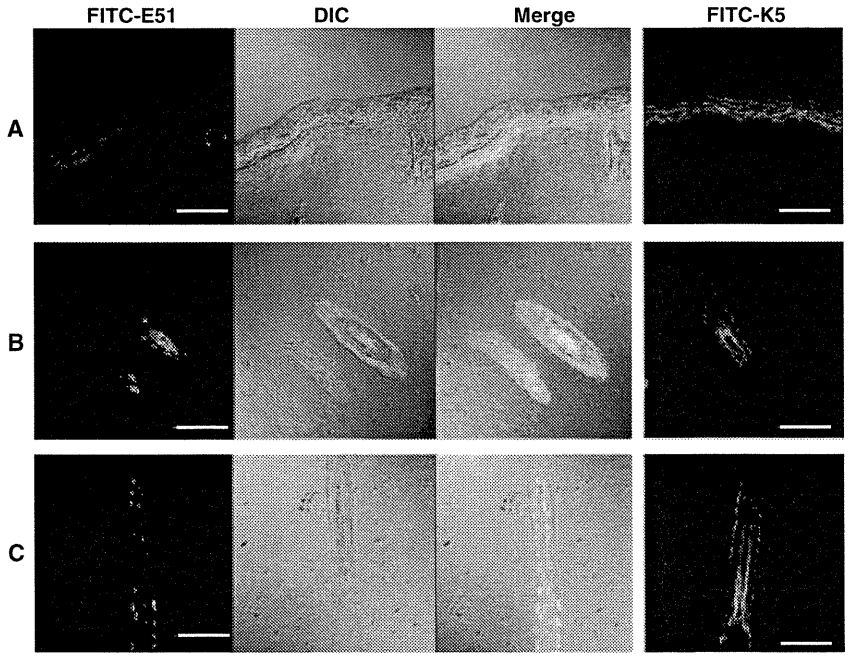

Fig. 7. *In situ* TGase activities detected with FITC-labeled peptides in the mouse skin epidermis and hair follicles. *In situ* activity of TGase 3 was detected under the observation at enlarged scale in the same reaction condition as described in the legend to Fig. 6. From left, FITC–pepE51 (1 μM), differential interference images and their merged images are aligned. FITC–pepK5 (1 μM) was paralleled in each experiment (right). (A) Skin epidermis, (B) transversal and (C) longitudinal sections of hair follicles. Bar represents 50 μm.

detection procedure for TGase *in situ* activity was not specific for TGase 3 in principle, because cadaverine is an amine substrate known to react with any active TGase.

Although aberrant TGase 1 activity has been reported in several skin diseases, as a consequence of genetic mutation [41,42], nothing has been reported regarding a TGase 3 defect in specific pathologies. Investigation of *in situ* activity of TGase 3 is a valuable method for elucidating the precise role of this isozyme in a variety of tissues and cells. Recently, detection of altered enzymatic activities in patients with TGase 1 mutation was successfully achieved using FITC–pepK5 [19]. Because this method is applicable for monitoring aberrant expression of TGase 3 activity, it will assist in the investigation unknown diseases which may be caused by TGase 3 mutations.

In conclusion, we have identified several preferred substrate sequences for TGase 3. The most reactive peptide sequence, E51, permitted the detection of *in vitro* and *in situ* activities of the active enzyme. In addition to pepK5, a specific preferred substrate peptide for TGase 1, pepE51 could become a useful tool to further characterize TGase activity and identify endogenous substrates in the skin and hair follicles.

Experimental procedures

Transglutaminases

For screening, human recombinant TGase 3 obtained by expression and purification from baculovirus-infected insect cells was used, as described previously [27]. For evaluation of the obtained sequences, recombinant human TGases 1, -2 and -3 and purified guinea-pig liver TGase were purchased from Zedira (Darmstadt, Germany) and Sigma (St. Louis, MO, USA). For the activation of TGase 3, the zymogen was proteolyzed by treatment with dispase (Roche, Mannheim, Germany). Human Factor XIII (Fibrogammin^{R}P; ZLB Behring, Marburg, Mannheim, Germany) was activated (Factor XIIIa) by treatment with bovine thrombin (Sigma).

Screening of preferred sequences from a phage-displayed peptide library

Screening was carried out as described previously, using an M13 PhD-12 phage-display system (New England Biolabs Inc., Ipswich, MA, USA) [15]. Briefly, $\sim 1.5 \times 10^{11}$ (first-round panning) phage clones were incubated at 37 °C with dispase-activated TGase 3 (1 ng·μL^{-1}) in 10 mM Tris/HCl (pH 8.0), 150 mM NaCl (TBS buffer) containing 1 mM dithiothreitol, 5 mM $CaCl_2$ and 5 mM bio-Cd [EZ-link™ 5-(biotinamido)pentylamine; Pierce Biotechnology, Rockford, IL, USA]. The catalytic reaction was stopped by the addition of EDTA. The phage particles were precipitated in the presence of poly-(ethylene glycol) and NaCl with salmon sperm DNA as a carrier. Next, phage clones that covalently incorporated bio-Cd were selected by affinity chromatography using mono-avidin gel (SoftLink™ Soft Release Avidin Resin; Promega Corp., Madison, WI, USA). After washing with TBS containing 0.1 or 0.5% Tween 20 and 2 mM EDTA and then with TBS, the bound phage particles were eluted by competition using 5 mM biotin in TBS buffer. The entire eluate was used to infect ER2738 host bacteria to amplify the phages. The phage particles were concentrated by precipitation with poly-(ethylene glygol)–NaCl and then used for subsequent rounds. After panning five times in all, DNA sequences of the displayed peptides of the selected phage clones were determined.

Construction of the expression vector for GST fusion proteins

The vector plasmid pET24d–GST(QN) was used to express modified GST, in which all the glutamine residues were substituted by asparagine residues, and fused with a peptide at the N-terminus and hexahistidine at the C-terminus [15]. The DNA of each phage was isolated and the sequences of the displayed 12-mer peptides were amplified by PCR. The amplified PCR products were digested and inserted into pET24d–GST(QN). To generate peptide mutants in which each amino acid was substituted to alanine, PCR-based mutagenesis was carried out.

Escherichia coli BL21(DE3)LysS or BL21(DE3)LysE was transformed with the plasmids and expression was induced by the addition of isopropyl β-D-thiogalactoside. Recombinant proteins were purified using TALON Metal Affinity Resin according to the manufacture's instructions (BD Bioscience, San Jose, CA, USA). The concentration of the purified protein was determined by quantification of the intensity for the separated bands in SDS/PAGE analysis using imaging software (MULTIGAUGE software; Fujifilm, Tokyo, Japan).

Evaluation of the preferred sequences using the recombinant proteins

The reactivities of recombinant GST(QN)-fusion proteins were evaluated by the incorporation of Dansyl-Cd (Sigma), a fluorescence-labeled pentylamine. Recombinant protein (200 ng·μL^{-1}) and 0.5 mM Dansyl-Cd were incubated in TBS containing 5 mM $CaCl_2$ and 1 mM dithiothreitol in the presence of activated TGase 3 (1 ng·μL^{-1}). Dimethylcasein (Sigma) was used as a positive control at a final concentration of 200 ng·μL^{-1}. The reaction mixture was incubated at 37 °C and then separated by 12.5% SDS/PAGE. A fluorograph of the gel was obtained by UV irradiation (254 nm) to visualize the amount of incorporated Dansyl-Cd. To quantify the results, the fluorescence intensity of each

product was analyzed using imaging software (MULTIGAUGE software).

Evaluation of synthetic peptides as a substrate

The 12-amino acid peptide corresponding to the E51 sequence (PPPYSFYQSRWV) was synthesized and biotinylated at the N-terminus (pepE51). A mutant peptide in which glutamine was substituted to asparagine was also synthesized (PPPYSFYNSRWV) and biotinylated as pepE51QN. TGase 1-, TGase 2- and Factor XIII-preferred substrate biotinylated peptides, being pepK5 (YEQHKLPSSWPF), pepT26 (HQSYVDPWMLDH) and pepF11 (DQMMLPWPAVAL), respectively, were used for comparison.

To evaluate the activity and specificity of the peptides, a microtiter plate assay was performed as described previously [32,33]. Spermine, as a primary amine, was immobilized covalently onto microplates. The enzyme reaction mixture, in a total volume of 100 μL, contained biotinylated peptide in the presence of the enzymes in an appropriate buffer (final concentration: 20 mM Tris/HCl, pH 8.3, 140 mM NaCl, 2.5 mM dithiothreitol, 15 mM $CaCl_2$). The microtiter plates were incubated at 37 °C for the indicated time intervals and the reaction was stopped by the addition of EDTA (50 mM at final concentration). The wells were then washed with a Tris-based buffer (10 mM Tris/HCl, pH 8.0, 150 mM NaCl, 0.1% Tween-20). The incorporated biotinylated peptides were detected using streptavidin-peroxidase (Rockland Immunochemicals Inc., Gilbertsville, PA, USA) and the peroxidase substrate 3,3′,5,5′-tetramethylbenzidine (Sigma).

Detection of *in situ* TGase activities in the mouse skin sections

Animal care and experiments were conducted according to the Regulations for Animal Experiments in Nagoya University.

Immediately after the mice had been killed by diethylether anesthetization, the skin was dissected and embedded in medium (Sakura Finetek, Tokyo, Japan) as a standard method. Frozen sections were dissected into 4–8 μm slices and kept frozen until use. Fluorescence-labeled peptides (FITC–pepE51, FITC–pepE51QN and FITC–pepK5) were synthesized.

For the reaction, sections were dried and then blocked by incubation in NaCl/P_i containing 1% BSA (Sigma) for 30 min at room temperature. Sections were incubated for 90 min with a solution containing 100 mM Tris/HCl (pH 8.0), 5 mM $CaCl_2$ or 5 mM EDTA and 1 mM dithiothreitol, in the presence of FITC-labeled peptide at 37 °C. After washing with NaCl/P_i three times, anti-fading solution was mounted onto the section with a cover-glass. Differential interference images and fluorescence were analyzed with a confocal laser-scanning microscope, LSM5 PASCAL (Zeiss, Göttingen, Germany). For hematoxylin and eosin staining, the tissue section was fixed, then stained using standard methods and analyzed with a microscope, BZ-8100 (Keyence, Osaka, Japan).

Acknowledgements

We greatly appreciate Dr Masatoshi Maki and Dr Hideki Shibata in our laboratory for providing valuable suggestions. This work was supported by a Grant-in-Aid for Scientific Research on Innovative Areas (No. 20200072) from the Ministry of Education, Sports, Science and Technology (MEXT, Japan) (to KH) and the Marie Curie Action RTN program 'Transglutaminase: role in pathogenesis, diagnosis and therapy' (TRACKS; contract No. MRTN-CT-2008-36032).

References

1 Griffin M, Casadio R & Bergamini CM (2002) Transglutaminases: nature's biological glues. *Biochem J* **368**, 377–396.
2 Lorand L & Graham RM (2003) Transglutaminases: crosslinking enzymes with pleiotropic functions. *Nat Rev Mol Cell Biol* **4**, 140–156.
3 Ichinose A (2001) Physiopathology and regulation of Factor XIII. *Thromb Haemost* **86**, 57–65.
4 Fésüs L & Piacentini M (2002) Transglutaminase 2: an enigmatic enzyme with diverstic functions. *Trends Biochem Sci* **27**, 534–539.
5 Fésüs L & Szondy Z (2005) Transglutaminase 2 in the balance of cell death and survival. *FEBS Lett* **579**, 3297–3302.
6 Telci D & Griffin M (2006) Tissue transglutaminase (TG2) – a wound response enzyme. *Front Biosci* **11**, 867–882.
7 Eckert RL, Sturniolo MT, Broome AM, Ruse M & Rorke EA (2005) Transglutaminase function in epidermis. *J Invest Dermatol* **124**, 481–492.
8 Hitomi K (2005) Transglutaminase in skin epidermis. *Eur J Dermatol* **15**, 313–319.
9 Zeeuwen PL (2004) Epidermal differentiation: the role of proteases and their inhibitors. *Eur J Cell Biol* **83**, 761–773.
10 Esposito C, Pucci P, Amoresano A, Marino G, Cozzolino A & Porta R (1996) Transglutaminase from rat coagulating gland secretion. Post-translational modification and activation by phosphatidic acids. *J Biol Chem* **271**, 27416–27423.
11 Candi E, Oddi S, Paradisi A, Terrinoni A, Ranalli M, Teofoli P, Citro G, Scarpato S, Puddu P & Melino G (2002) Expression of transglutaminase 5 in normal and pathologic human epidermis. *J Invest Dermatol* **119**, 670–677.

12 Pietroni V, Di Giorgi S, Paradisi A, Ahvazi B, Candi E & Melino G (2008) Inactive and highly active, proteolytically processed transglutaminase-5 in epithelial cells. *J Invest Dermatol* **128**, 2760–2766.
13 Esposito C & Caputo I (2005) Mammalian transglutaminases: identification of substrates as a key to physiological function and physiological relevance. *FEBS J* **272**, 615–631.
14 Facchiano A & Facchiano F (2009) Transglutaminases and their substrates in biology and human diseases: 50 years of growing. *Amino Acids* **36**, 599–614.
15 Sugimura Y, Hosono M, Wada F, Yoshimura T, Maki M & Hitomi K (2006) Screening for the preferred substrate sequence of transglutaminase using a phage-displayed peptide library: identification of peptide substrates for TGase 2 and Factor XIIIa. *J Biol Chem* **281**, 17699–17706.
16 Sugimura Y, Hosono M, Kitamura M, Tsuda T, Yamanishi K, Maki M & Hitomi K (2008) Identification of preferred substrate sequences for transglutaminase 1-development of a novel peptide that can efficiently detect cross-linking enzyme activity in the skin. *FEBS J* **275**, 5667–5677.
17 Sugimura Y, Yokoyma K, Nio N, Maki M & Hitomi K (2008) Identification of preferred substrate sequences of microbial transglutaminase from Streptomyces mobaraensis using a phage-displayed peptide library. *Arch Biochem Biophys* **477**, 379–383.
18 Hitomi K, Kitamura M & Sugimura Y (2009) Preferred substrate sequences for transglutaminase 2: screening using a phage-displayed peptide library. *Amino Acids* **36**, 619–624.
19 Akiyama M, Sakai K, Yanagi T, Fukushima S, Ihn H, Hitomi K & Shimizu H (2010) Transglutaminase 1 preferred substrate peptide K5 is an efficient tool in diagnosis of lamellar ichthyosis. *Am J Pathol* **176**, 1592–1599.
20 Sugimura Y, Ueda H, Maki M & Hitomi K (2007) Novel site-specific immobilization of a functional protein using a preferred substrate sequence for transglutaminase 2. *J Biotechnol* **131**, 121–127.
21 Kim HC, Lewis MS, Gorman JJ, Park SC, Girard JE, Folk JE & Chung SI (1990) Protransglutaminase E from guinea pig skin. Isolation and partial characterization. *J Biol Chem* **265**, 21971–21978.
22 Kim I-G, Gorman JJ, Park S-C, Chung S-I & Steinert PM (1993) The deduced sequence of the novel protransglutaminase E (TGase3) of human and mouse skin. *J Biol Chem* **268**, 12682–12690.
23 Kalinin AE, Kajava AV & Steinert PM (2002) Epithelial barrier function: assembly and structural features of the cornified envelop. *Bioessays* **24**, 789–800.
24 Candi E, Schmidt R & Melino G (2005) The cornified envelope: a model of cell death in the skin. *Nat Rev Mol Cell Biol* **6**, 328–340.
25 Cheng T, Hitomi K, van Vlijmen-Willems IM, Jongh G, Yamamoto K, Nishi K, Watts C, Reinheckel T, Schalkwijk J & Zeeuwen PM (2006) Cystatin M/E is a high affinity inhibitor of cathepsin V and the short chain form of cathepsin L by a reactive site that is distinct from the legumain-binding site. A novel clue for the role of cystatin M/E in epidermal cornification. *J Biol Chem* **281**, 15893–15899.
26 Zeeuwen PM, Cheng T & Schalkwijk J (2009) The biology of cystatin M/E and its cognate target protease. *J Invest Dermatol* **129**, 1327–1338.
27 Hitomi K, Kanehiro S, Ikura K & Maki M (1999) Characterization of recombinant mouse epidermal-type transglutaminase (TGase 3): regulation of its activity by proteolysis and guanine nucleotides. *J Biochem (Tokyo)* **125**, 1048–1054.
28 Hitomi K, Horio Y, Ikura K, Yamanishi K & Maki M (2001) Analysis of epidermal-type transglutaminase expression in mouse tissues and cell lines. *Int J Biochem Cell Biol* **33**, 491–498.
29 Ahvazi B, Boeshans KM, Idler W, Baxa U & Steinert P (2003) Roles of calcium ions in the activation and activity of the transglutaminase 3 enzyme. *J Biol Chem* **278**, 23834–23841.
30 Hitomi K, Presland RB, Nakayama T, Fleckman P, Dale BA & Maki M (2003) Analysis of epidermal-type transglutaminase (transglutaminase 3) in human stratified epithelia and cultured keratinocytes using monoclonal antibodies. *J Dermatol Sci* **32**, 95–103.
31 Ahvazi B, Boeshans KM & Rastinejad F (2004) The emerging structural understanding of transglutaminase 3. *J Struct Biol* **147**, 200–207.
32 Alea MP, Kitamura M, Martin G, Thomas V, Hitomi K & El Alaoui S (2009) Development of a highly sensitive and specific colorimetric assay for the measurement of TGase 2 cross-linking activity. *Anal Biochem* **389**, 150–156.
33 Hitomi K, Kitamura M, Alea MP, Ceylan I, Thomas V & El Alaoui S (2009) A specific colorimetric assay for measuring of transglutaminase 1 and Factor XIII activities. *Anal Biochem* **394**, 281–283.
34 Brown DR, Kitchin D, Qadadri B, Neptune N, Batteiger T & Ermel A (2006) The human papillomavirus type 11 E1^E4 protein is a transglutaminase 3 substrate and induces abnormalities of the cornified cell envelope. *Virology* **345**, 290–298.
35 Tarcsa E, Candi E, Kartasova T, Idler WW, Marekov LN & Steinert PM (1998) Structural and transglutaminase substrate properties of the small proline-rich 2 family of cornified cell envelope proteins. *J Biol Chem* **273**, 23297–23303.
36 Candi E, Tarcsa E, Idler WW, Kartasova T, Marekov LN & Steinert PM (1999) Transglutaminase cross-linking properties of the small proline-rich 1 family of